Received: 7 June 2019 | Revised: 29 January 2020 | Accepted: 5 February 2020

DOI: 10.1111/psyp.13576

ORIGINAL ARTICLE

PSYCHOPHYSIOLOGY SPR WILEY

The quest for the genuine visual mismatch negativity (vMMN): Event-related potential indications of deviance detection for low-level visual features

Alie G. Male[1] | **Robert P. O'Shea**[1,2,3] | **Erich Schröger**[2] | **Dagmar Müller**[2] | **Urte Roeber**[1,2] | **Andreas Widmann**[2,4]

[1]Discipline of Psychology, College of Science, Health, Engineering and Education, Murdoch University, Perth, WA, Australia

[2]Institute of Psychology, Leipzig University, Leipzig, Germany

[3]Discipline of Psychology, School of Health and Human Sciences, Southern Cross University, Coffs Harbour, NSW, Australia

[4]CBBS Research Group Neurocognitive Development, Leibniz Institute for Neurobiology, Magdeburg, Germany

Correspondence
Andreas Widmann, Institute of Psychology, Leipzig University, Neumarkt 9–19, Leipzig, DE 04109, Germany.
Email: widmann@uni-leipzig.de

Funding information
Deutscher Akademischer Austausch Dienst (DAAD), Grant/Award Number: 91651341; German Research Foundation (DFG), Grant/Award Number: SCHR 375/25-1

Abstract

Research shows that the visual system monitors the environment for changes. For example, a left-tilted bar, a *deviant*, that appears after several presentations of a right-tilted bar, *standards*, elicits a *classic* visual mismatch negativity (vMMN): greater negativity for deviants than standards in event-related potentials (ERPs) between 100 and 300 ms after onset of the deviant. The classic vMMN is contributed to by adaptation; it can be distinguished from the *genuine* vMMN that, through use of control conditions, compares standards and deviants that are equally adapted and physically identical. To determine whether the vMMN follows similar principles to the auditory mismatch negativity (MMN), in two experiments we searched for a genuine vMMN from simple, physiologically plausible stimuli that change in fundamental dimensions: orientation, contrast, phase, and spatial frequency. We carefully controlled for attention and eye movements. We found no evidence for the genuine vMMN, despite adequate statistical power. We conclude that either the genuine vMMN is a rather unstable phenomenon that depends on still-to-be-identified experimental parameters, or it is confined to visual stimuli for which monitoring across time is more natural than monitoring over space, such as for high-level features. We also observed an early deviant-related positivity that we propose might reflect earlier predictive processing.

KEYWORDS

adaptation, attention, contrast, EEG, electroencephalography, ERP, event-related potentials, eye movement, Gabor patch, orientation, phase, spatial frequency, vision, visual mismatch negativity, vMMN

1 | INTRODUCTION

Sights, sounds, touches, tastes, and smells flood our senses at every moment. Yet, we do not experience all this information, if only because it would require lots of energy for our brains to process it completely. Instead, our brains preferentially process unexpected changes in sensory input.

One signature of the processing of changes is the mismatch negativity (MMN), discovered by Näätänen, Gaillard, and Mäntysalo (1978) in the auditory modality. It

is a brain response to a rare, unpredicted, different, *deviant* tone after a series of identical *standard* tones, a so-called *oddball sequence*. One derives the MMN by comparing event-related potentials (ERPs) from deviants and standards collected with electroencephalography (EEG). It occurs sometime between 100 and 300 ms after the onset of the deviant.

Various kinds of deviants produce the MMN, from simple feature deviants such as the pitch, intensity, or duration of tones, to increasingly complex and abstract deviants, such as unexpected repetition in a series of ever-changing tones. For a review, see Näätänen, Paavilainen, Rinne, and Alho (2007).

Analogs of the MMN have been reported for other sensory modalities, including olfaction (Krauel, Schott, Sojka, Pause, & Ferstl, 1999), touch (Kekoni et al., 1997), and vision (Cammann, 1990; Czigler & Csibra, 1990). Our concern in this article is with vision: the visual mismatch negativity (vMMN). There is a presupposition that all analogs of the MMN should adhere to at least four principals:

1. The MMN reflects processes beyond neural refractoriness or adaptation (see O'Shea, 2015 for a critical discussion of the terminology) such as memory comparison (Näätänen, Jacobsen, & Winkler, 2005), model updating (Winkler, Karmos, & Näätänen, 1996), lateral inhibition (May & Tiitinen, 2010), or prediction error (Garrido, Kilner, Stephan, & Friston, 2009). Paavilainen, Alho, Reinikainen, Sams, and Näätänen (1991) called this the "genuine" (p. 477) MMN to distinguish it from the *classic* MMN contributed to by adaptation.
2. The MMN occurs in response to regularity violations in well-isolated, low-level, physiologically plausible, sensory features (Näätänen et al., 2007).
3. The MMN may not require attention (Näätänen, 1992).
4. The MMN is not due to physical differences of the stimuli (Kujala, Tervaniemi, & Schröger, 2007).

Here, we discuss whether these presuppositions are supported by vMMN research. Although there exist hundreds of vMMN studies on many different types of deviants, we focused on changes in orientation, contrast, phase, and spatial frequency because, according to Graham (1989), these are among the key dimensions for describing the appearance of images and they are processed in the visual cortex (V1) or earlier.[1]

We reviewed all studies that we found examining vMMN to these low-level visual features and list relevant parameters and results in Table 1. We then developed a paradigm to test these presuppositions for vMMN.

In Table 1, entries appear chronologically within each deviant feature: orientation, contrast, and spatial frequency (we were unable to find any studies that varied phase). If a single study conducted more than one experiment, we give the details of each separately. Likewise, if a single experiment tested two features or conditions separately, we give details for each separately.

For each experiment or condition, we provide details about:

- Number (N) of participants contributing to the final data set.
- The stimulus(i) used.
- Difference between the deviant and standard in units measured. In studies with more than one deviant size, we give the smallest difference that produced the vMMN.
- Whether the participant's task was visual, auditory, or manual.
- What participants attended to in order to perform their task.
- Whether there was any control comparing deviants with physically identical standards. This can be achieved by having deviants and standards *reverse roles* in different blocks, by including a block omitting standards (*deviant alone*, i.e., no stimulus was presented instead of the standards), by including a *deviant block* comprising only deviants, or by including a *standard block* comprising only standards.
- Whether there was any control for adaptation (typically including control for physical differences), such as the *equiprobable* control or the *cascadic* control (see later).
- The latency of maximum amplitude of the vMMN (in ms).
- The electrode or region of interest.
- The mean amplitude of the classic, deviant (D) minus standard (S) vMMN, containing adaptation effects as well as genuine deviance effects (in μV).
- The mean amplitude of the genuine, D minus control (C) vMMN (μV; where applicable). We also show, with footnote e, whether there was a statistically significant adaptation effect (controls vs. standards).
- The effect size of the classic vMMN (in Cohen's *d*; Cohen, 1977).
- The effect size of the genuine vMMN (*d*; where applicable).

We give details of the condition that produced the largest (i.e., most negative) genuine vMMN. Amplitudes in red italics were not statistically significant. Where a piece of information was not reported, could not be calculated from the information available, or was not applicable (e.g., there was no control for adaptation), we leave a blank. We preserved

[1]This is not a comprehensive list of low-level visual features. Others include wavelength, luminance, direction of movement, and binocular disparity.

TABLE 1 VMMN research in which the deviant differs from standards in orientation, contrast, or spatial frequency

Study	*N*	Stimulus(i)	Smallest difference	Task modality	Attention on	Physical control[a]	Adaptation control[a]	Latency of maximum negativity (ms)	Electrode or ROI	Classic vMMN amplitude (μV)	Classic effect size (Cohen's *d*)	Genuine vMMN amplitude (μV)	Genuine effect size (Cohen's *d*)
Orientation													
Fu et al. (2003)	12	Square-wave grating	90°	Visual	Spatial frequency of grating	Reverse roles		192	Occipital	−1.90[c]			
Astikainen, Ruusuvirta, Wikgren, and Korhonen (2004)	8	Light bar	90°	Auditory	Words	Deviant alone		180[b]	Pz	−1.28[c]	−1.79		
Astikainen et al. (2008)	10	Dark bar	36°	Auditory	Words	Reverse roles	Equiprobable	195[b]	Occipital	−1.13[c]	−2.06	−0.69[c]	−0.79
Czigler and Pató (2009), Experiment 1	14	Grid pattern	90°	Visual	Quadrangle width			280[b]	Right posterior	−1.01[c]	−0.64		
Kimura et al. (2009)	12	Grey bar	36°	Visual	Bar-edges	Reverse roles	Equiprobable	225[b]	T6(P8)	−2.25[c]	−1.60	−1.60[c,e]	−1.78
Czigler and Sulykos (2010)	24	Peripheral line segments	30°	Visual	Color of central line segment	Reverse roles		166	Oz	−0.60	−0.87		
Sulykos and Czigler (2011)	12	Gabor patches	90°	Visual	Spaceship task[d]	Reverse roles		130	Oz	−2.55	−1.60		
Kimura and Takeda (2013)	22	Grey bars	33°	Visual	Fixation dot	Reverse roles	Equiprobable	226[b]	PO8	−2.62	−2.39	−0.93[e]	−0.63
Shi et al. (2013)	12	Red rectangles	90°	Visual	Fixation cross			200[b]	Occipito-temporal	−1.60			
Sulykos, Kecskés-Kovács, and Czigler (2013)	12	Gabor patches	30°	Visual	Spaceship task[d]		Equiprobable	210[c]	Parieto-occipital			*−0.05*[c]	
Takács, Sulykos, Czigler, Barkaszi, and Balázs (2013), Experiment 1	17	Gabor patches	50°	Visual	Fixation dot	Reverse roles		134	Parieto-occipital	−0.65			
Takács et al. (2013), Experiment 2	19	Gabor patches	90°	Visual	Fixation dot	Reverse roles		148	Parieto-occipital	−0.84			
Kimura and Takeda (2014), Experiment 1	23	Grey bar	22°	Manual	Button press	Reverse roles		225[b]	Right occipito-temporal	−1.19	−1.30		
Kimura and Takeda (2014), Experiment 2	21	Grey bar	22°	Manual	Button press	Reverse roles		265[b]	Right occipito-temporal	−0.92	−0.97		
Qian et al. (2014)	14	Red rectangles	90°	Visual	Fixation cross			200	Occipito-temporal	−1.13			
Farkas, Stefanics, Marosi, and Csukly (2015)	27	Gabor patches	90°	Visual	Fixation cross	Reverse roles		145[b]	Saggital parieto-occipital	−0.30	−0.68		
Kimura and Takeda (2015)	22	Grey bars	33°	Visual	Fixation dot	Reverse roles	Equiprobable	202[b]	PO8			−1.16[e]	−0.72
Bodnár, File, Sulykos, Kecskés-Kovács, and Czigler (2017), Experiment 1	17	Line texture	90°	Visual	Spaceship task[d]	Reverse roles		124	Parieto-Occipital	−1.44	1.52		
File et al. (2017), Experiment 1	15	Line texture	36°	Visual	Spaceship task[d]	Reverse roles	Cascadic	144	Parieto-occipital	−0.67	−1.15	*−0.09*	−0.26
Pesonen et al. (2017)	16	Dark bar	36°	Auditory	Words			210	Occipital	−1.02[c]			
Yan et al. (2017)	15	Black arrows	90°	Visual	Fixation cross	Reverse roles		200[c]	Parieto-occipital	−2.60[c]			
Smout et al. (2019)	24	Gabor patches	20°	Visual	Spatial frequency of Gabor patch	Reverse roles	Equiprobable	240[c]	PO8	−0.97[c]		−0.75[c]	
Smout et al. (2019)	24	Gabor patches	20°	Visual	Fixation dot	Reverse roles	Equiprobable	170[c]	PO8	+0.10[c]		*−0.05*[c]	
Contrast													
Nyman et al. (1990)	9	Square-wave gratings	−0.48 M	Visual	Fixation dot	Reverse roles		150[b]	Oz	−0.28	−0.11		
Wei et al. (2002)	12	Color scenery		Auditory or Visual	Contrast increment			152[b]	O2	−1.65[c]			

(Continues)

TABLE 1 (Continued)

Study	*N*	Stimulus(i)	Smallest difference	Task modality	Attention on	Physical control[a]	Adaptation control[a]	Latency of maximum negativity (ms)	Electrode or ROI	Classic vMMN amplitude (μV)	Classic effect size (Cohen's *d*)	Genuine vMMN amplitude (μV)	Genuine effect size (Cohen's *d*)
Spatial frequency													
Tales et al. (1999), Experiment 1	12	White vertical rectangles	+0.6 cpd	Visual	Fixation square			325[b]	O2	−4.00[c]			
Tales et al. (1999), Experiment 2	12	White vertical rectangles	−0.6 cpd	Visual	Fixation square			325[b]	O1	−1.86[c]			
Tales et al. (2002)	24	White vertical rectangles	−0.6 cpd	Visual	Fixation square			325[b]	O2	−3.40[c]			
Heslenfeld (2003)	14	Vertical gratings	1.72 cpd	Visual	Visuomotor task	Reverse roles		150[b]	Oz	−1.10	−2.10		
Kenemans et al. (2003)	12	Vertical square-wave gratings	1.8 cpd	Visual	Fixation cross	Deviant alone		135	Oz	−1.19[c]			
Stagg et al. (2004)	12	White vertical rectangles	0.6 cpd	Visual	Fixation square	Reverse roles		305[b]	Occipital	−3.73[c]			
Maekawa et al. (2005)	7	Windmill pattern	18 vanes	Auditory and Visual	Story and target windmill	Reverse roles		245[c]	Oz	−3.47[c]	−2.13		
Tales and Butler (2006)	11	White vertical rectangles	+0.6 cpd	Visual	Fixation square			300[b]	T6(P8)	−3.90[c]			
Maekawa et al. (2009), Experiment 1	10	Windmill pattern	18 vanes	Auditory	Story	Deviant block		252[c]	Oz	−6.33[c]			
Maekawa et al. (2009), Experiment 2	8	Windmill pattern	18 vanes	Auditory	Story	Standard block		232[c]	Oz	−2.19[c]	−1.20		
Kenemans, Hebly, Heuvel, and Grent-T-Jong (2010)	16	Vertical square-wave gratings	1.8 cpd	Visual	Fixation cross	Reverse roles		160[b]	Oz	−0.50[c]	−0.63		
Chang et al. (2011)	14	White vertical rectangles	0.6 cpd	Visual	Fixation square	Reverse roles	Equiprobable	200[b]	Parieto-occipital	−0.95[c]	−3.06	−1.25[c]	−3.13
Sulykos and Czigler (2011)	12	Gabor patches	4 cpd	Visual	Spaceship task[d]	Reverse roles		136	Oz	−1.18	−1.10		
Cleary et al. (2013)	20	Horizontal square-wave gratings	−6 cpd	Visual	Fixation cross			165[b]	O2	−2.06			
Maekawa et al. (2013)	20	Windmill pattern	18 vanes	Visual	Target windmill	Reverse roles		280[b]	Oz	−1.25[c]			
Stothart and Kazanina (2013)	39	White vertical rectangles	+0.6 cpd	Visual	Fixation square			222[c]	Parieto-occipital	−0.66[c]			
Hedge et al. (2015)	20	Vertical square-wave gratings	6 cpd	Visual	Fixation square	Reverse roles		265[b]	Parieto-occipital	−0.94	−0.55		
Bodnár et al. (2017), Experiment 2	19	Windmill pattern	6 vanes	Visual	Fixation dot	Reverse roles		203	Occipital	−1.73	−0.78		
File et al. (2017), Experiment 2	23	Windmill pattern	6 vanes	Visual	Spaceship task[d]	Reverse roles	Equiprobable	269	Occipital	−1.46	−1.17	−1.49	−1.19

[a]See text for explanation of categories.

[b]This value represents the midpoint of the time window used to calculate mean amplitude.

[c]This value was calculated from the studies' figures.

[d]The task field occupied an area of the visual field opposite that of the stimuli of interest.

[e]This study also tested for and reported a statistically significant adaptation effect (controls vs. standards).

[f]Participants navigated a moving spaceship through a canyon while avoiding and catching color-determined targets.

the sign of Cohen's *d*s: all reported negativities should have negative *d*s.

Next, we relate vMMN to the four MMN presuppositions.

1.1 | Adaptation

ERP responses to repeated stimuli are typically smaller in amplitude, reflecting adaptation. Therefore, the greater negativity to deviants could come solely or partly from adaptation by the repetition of standards in oddball sequences (for thorough discussion see May & Tiitinen, 2010).

To disentangle adaptation from genuine detection of deviants, Schröger and Wolff (1996) developed an *equiprobable* control. In control blocks, different stimuli, including stimuli physically identical to the deviant, appear in random order, preventing any regularity, each with a frequency equal to that of the deviant in oddball blocks, equalizing adaptation. Schröger and Wolff argued that the comparison of deviants and physically identical control stimuli reflect the detection of regularity violations. We used this control in Experiment 1.

Ruhnau, Herrmann, and Schröger (2012) argued that with the equiprobable control adaptation is potentially overestimated. They proposed a block in which the stimulus changes regularly in a feature of interest (e.g., orientation) from trial to trial, which they called the cascadic-control block. This allows an expectation of the control stimulus to be established while keeping an adaptation level comparable with the one for the deviant in the oddball block. We used this control in Experiment 2 to ensure our findings were unrelated to overestimated adaptation.

Table 1 shows that only 10 out of 44 (23%) vMMN experiments or conditions used either control, seriously limiting the conclusions we can draw from the literature about the genuine vMMN.

1.2 | Isolation and physiological plausibility of feature manipulations

Most stimuli used for vMMN research are not suited for manipulating low-level visual features. For example, a bar contains one orientation along its length and another, at right angles, at its end. Any stimulus with sharp edges necessarily stimulates wide bands of spatial frequencies.

Gabor patches, on the contrary, are ideal for isolating single low-level features. A Gabor patch of a particular mean luminance comprises a sinusoidal grating of a particular frequency, phase, and orientation whose contrast reduces with distance from the center of the grating by a Gaussian function (size expressed as the standard deviation [*SD*] in degrees of visual angle). That is, the orientation, spatial frequency, and luminances of a Gabor patch are as specified, without any other orientations, spatial frequencies, or luminances. Most importantly, by using Gabor patches, we can manipulate isolated features without affecting other low-level visual features.

Gabor patches are physiologically plausible because their profiles resemble the receptive fields of simple cells in the visual cortex (Daugman, 1985; Field & Tolhurst, 1986; Fredericksen, Bex, & Verstraten, 1998). A simple cell's receptive field has a preferred orientation and spatial frequency, dictating the stimuli to which it responds. An appropriate Gabor patch will ideally excite that cell.

Only eight vMMN experiments or conditions used Gabor patches (18%), again limiting the conclusions, we can draw from the literature about vMMN to isolated, single features.

1.3 | Attention

One of the defining features of the MMN is that it occurs without attention. Inherent differences between the sensory modalities make it difficult to equate the allocation of attention across auditory and visual modalities. In vision, the eyes must be on the stimulus even if it is not task-relevant; in audition, the ears cannot be other than on the stimulus.

Table 1 shows the various ways in which attention has been manipulated in vMMN research. Attention can be on the stimulus of interest (e.g., Kimura, Katayama, Ohira, & Schröger, 2009), on some unrelated distractor stimulus (e.g., Sulykos, Kecskés-Kovács, & Czigler, 2013), or on stimulation in another modality (e.g., Astikainen, Lillstrang, & Ruusuvirta, 2008). To conclude whether the vMMN is preattentive—as the auditory MMN is thought to be—the stimulus of interest should not be task-relevant. However, one must ensure that participants are looking consistently at the stimulus of interest without attending to it. We find that 27 experiments or conditions (61%) used a fixation stimulus that is not part of the stimuli of interest, solving this problem.

1.4 | Comparison of physically identical stimuli

Physically different stimuli may elicit different ERPs, making it impossible to attribute differences to the detection of regularity violations. One can compare physically identical stimuli by administering oddball blocks in which standards and deviants reverse roles. Other methods, such as administering blocks containing only deviants, produce unexpectedly large classic vMMNs (e.g., Maekawa et al., 2005). Although 28 (63%) experiments and conditions compared physically identical stimuli, only 10 (23%) also had an appropriate control for adaptation, again seriously limiting the conclusions, we can draw from the literature about the genuine vMMN.

1.5 | Other issues

Table 1 also shows two inconsistencies in research into low-level deviants:

1. *vMMN peak latency*. vMMN peak latencies have been reported as early as 130 ms (*orientation*: Sulykos & Czigler, 2011) or as late as 305 ms (*spatial frequency*: Stagg, Hindley, Tales, & Butler, 2004). Inconsistencies exist even with similar stimuli. For example, Maekawa et al. (2005) reported a vMMN to windmill-like patterns at 185 ms, whereas File et al. (2017) reported a vMMN to the same patterns at least 70 ms later. Such timing differences are difficult to reconcile, unless we accept that other processes may be affecting one of the reported vMMNs.
2. *Replicability of some vMMNs*. Five studies reported a genuine orientation vMMN, whereas three showed no significant genuine vMMN. Two studies found that spatial frequency deviants produced a vMMN only when deviants had higher spatial frequencies than the standard (File et al., 2017; Hedge et al., 2015). File et al. manipulated spatial frequency by changing the number of vanes in their sharp-edged radial gratings—windmill-like patterns—on deviant trials and argued that the deviant with fewer vanes did not produce a vMMN, because it was less complex. However, increasing the number of vanes also confoundingly increases the number of orientations in the stimulus.

These inconsistencies suggest that some other facet may predict whether a genuine vMMN occurs. A key question is whether low-level feature deviants yield a vMMN when, in the same experiment, one controls for adaptation, uses physiologically plausible stimuli isolating the manipulated feature, manipulates task-irrelevant stimuli while ensuring the eyes are on the stimulus, and compares physically identical stimuli. We address this question in two experiments.

1.6 | Experiment 1

We replicated an experiment by Kimura et al. (2009) who used the equiprobable control and reported a genuine orientation vMMN. We selected this study because it was methodologically sound, reported large effects that were very well-controlled for adaptation (a necessity when one is interested in the underlying mismatch mechanisms), and because one of us (ES) was involved in it. Kimura et al. used bars and had their participants press a button whenever the ends of the bars had rounded corners. We added conditions to tease apart potential contributors to the vMMN they reported by testing the same orientation change with Gabor patches and by testing conditions in which the participants' attention/task was not on the ends of the stimuli but on a central fixation dot. We also measured where participants looked on the stimuli using a remote eye-tracker.

1.7 | Experiment 2

We tested orientation, contrast, phase, and spatial frequency deviants with Gabor patches using a multi-feature paradigm (Näätänen, Pakarinen, Rinne, & Takegata, 2004) and the cascadic control (Ruhnau et al., 2012). In the multi-feature paradigm, a feature of the stimulus, rather than the whole stimulus, can change to give a deviant for that feature and a standard for others. Similarly, all other stimuli are standards for that feature even though they may be deviants for others. One complete standard separates each deviant and each deviant feature appears once per set of four standard/deviant pairs of four trials in a pseudo-randomized order. This gives a probability of any feature similar to that of a traditional oddball block (here 12.5%). The advantage of this approach is that one can test multiple deviants within a short time.

2 | EXPERIMENT 1

2.1 | Introduction

We replicated Kimura et al.'s (2009) study of orientation deviants using single bars (Figure 1a, I). We added three conditions, giving a 2 × 2 design of stimulus type: *bar* condition (Figure 1a, I and II) versus *Gabor* condition (Figure 1a, III and IV), and whether attention was on the edges of the stimuli to give the *edge* condition (Figure 1a, I and III) versus whether attention was on a central fixation dot to give the *fixation* condition (Figure 1a, II and IV). We also measured participants' eye positions, fearing that when participants were attending to the bar ends their eyes might wander toward them, even though we instructed them to keep their eyes in the center of the screen (as Kimura et al., 2009, did).

2.2 | Method

2.2.1 | Participants

Using G*Power (Faul, Erdfelder, Buchner, & Lang, 2009; Faul, Erdfelder, Lang, & Buchner, 2007), we estimated the sample size needed to achieve a power of 0.9 given the effect size found by Kimura et al. (2009): 5 participants. To optimize the likelihood of finding their effect, we tested 24 self-declared healthy adults (10 males, 20 right-handed) with normal or corrected-to-normal vision for a power of 0.99.

Mean age was 24.20 years with a range from 19 to 49. The Murdoch University Ethics Committee approved the experiments (2015/208). All participants provided their written informed consent and were free to withdraw from the experiment at any time. Participants received monetary compensation or course credit in return for participation. The experiment took place in the BioCog laboratories of Leipzig University.

2.2.2 | Apparatus

Participants sat in an electrically shielded, sound-attenuated, and light-attenuated chamber. They viewed stimuli on a photometrically linearized, 19-inch, color, CRT monitor (Viewsonic G90fB) from 60 cm. The monitor showed 1,024 × 768 pixels at a refresh rate of 100 Hz; it was the only source of light. A forehead-and-chin rest stabilized participants' heads. Participants gave their responses by pressing a key on a 4-key response pad connected to a response registration device (RTBox; Li, Liang, Kleiner, & Lu, 2010). A PC with Ubuntu Linux v16.04.1, Octave v4.0, and Psychophysics Toolbox 3.0.14 (Brainard, 1997; Kleiner, 2013; Pelli, 1997) presented stimuli and recorded responses. We used an EyeLink 1000 (SR Research, Ottawa, Ontario, Canada) remote eye-tracker.

2.2.3 | Stimuli

In two conditions, we presented bar stimuli; in the remaining two conditions, we presented Gabor stimuli. For the bar stimuli, we used the original stimuli from Kimura et al. (2009): rectangular grey bars with a length of 3° visual angle and a width of 0.5° visual angle. The bars had a luminance of 41.7 candles per square meter (cd/m^2) (Kimura et al., 2009: 42 cd/m^2) on a black background with a luminance of 0.01 cd/m^2. This gave them a Michelson contrast greater than 0.99. Non-target bars had right-angled corners at their ends; target bars had rounded corners (Figure 1a, I).

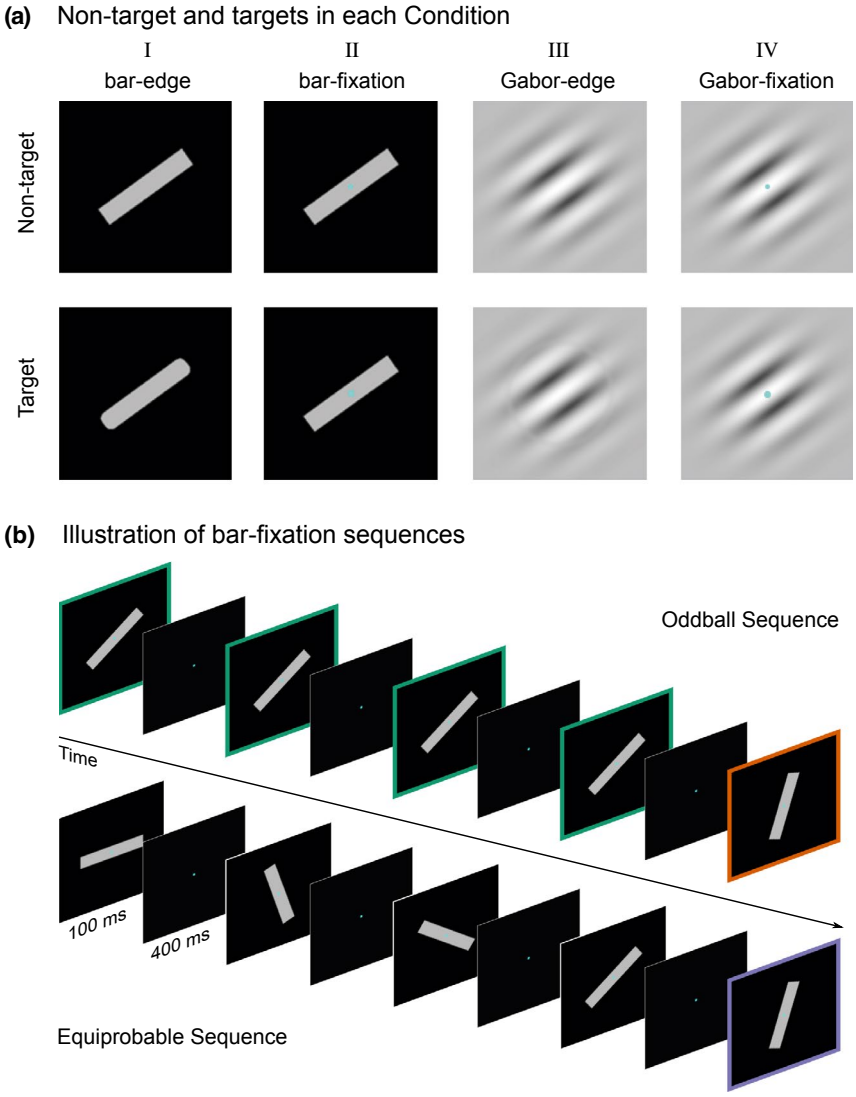

FIGURE 1 Experiment 1. (a) Examples of stimuli for the 2 × 2 design of Experiment 1. In this case, the orientation of non-target stimuli (top panel) and target stimuli (bottom panel) is 36° anticlockwise from horizontal, 0°. Stimuli were either bars (left two columns: I and II) or Gabor patches (right two columns: III and IV). Participants either paid attention to the edges of the stimuli (edge task: columns I and III) or to a fixation dot (fixation task: columns II and IV). (b) Example of an oddball and an equiprobable control block for the bar-fixation condition. The deviant (in orange) and control (in purple) have a probability of 20%. In the oddball block, the standards (in green) have a probability of 80%

Gabor patches comprised a grating with a Michelson contrast of 0.99, a phase of 0.5π radians (i.e., a white peak at the center of the monitor), a spatial frequency of 1 cycle per degree (cpd) of visual angle, a mean luminance of 41.8 cd/m^2, and a peak luminance of 83.8 cd/m^2. The background had the same mean luminance. The Gaussian envelope had a *SD* of 1° visual angle.

Target Gabor patches in the edge condition had a circular, raised-cosine-window-shaped margin with a radius of 1.5° visual angle, where the contrast was reduced from full to 30% over 0.33°. It appeared as a grey ring (Figure 1a, III). Bar and Gabor stimuli had an orientation of 0°, 36°, 72°, 108°, or 144° anticlockwise from horizontal.

In the fixation conditions, bars and Gabor patches had a central, cyan, circular fixation dot with a diameter of 0.13° visual angle and a luminance of 33.1 cd/m^2 for the bars and 64.2 cd/m^2 for the Gabor patches (Figure 1a, II and IV). Target fixation dot diameter was 0.26° visual angle. In the edge conditions, there was no fixation dot.

2.2.4 | Procedure

There were two stimulus and two task conditions each, arranged in a 2 × 2 design giving four conditions (see Figure 1a). We counterbalanced the order of conditions across participants.

Each condition started with written instructions and consisted of 12 blocks each taking 55 s to complete its 110 trials. Participants were free to take breaks between blocks. To complete all 48 blocks took an average of 44 min. Ten of the 12 blocks per condition were oddball blocks and 2 were equiprobable control blocks. We randomized block order within each condition afresh for each participant and condition. Oddball blocks had 80% of standard trials and 20% of deviant trials (see Figure 1b).

Standard and deviant trials were pseudo-randomized for each participant and block except that at least two standards separated deviants. Each of the five possible orientations was a standard in two oddball blocks. In one of these, deviant orientation was +36° from that of the standards, in the other it was −36°. Equiprobable blocks contained 20% each of the five possible orientations in pseudo-randomized order: there were no repetitions of orientation within these blocks.

Stimulus onset asynchrony (SOA) was 500 ms, featuring a 400 ms inter-stimulus-interval (ISI). In fixation conditions, the fixation dot was always present (see Figure 1b). All stimuli appeared at the center of the screen. We instructed participants to look at the center of the screen during all trials, whether there was a fixation dot or not. The first block of each condition and any blocks following a break began with a 9-point eye-tracker calibration and validation routine.

In all conditions, 9% of the stimuli (8 standards, 2 deviants in oddball blocks; 10 in equiprobable blocks) were targets. We asked participants to press a key as fast as possible with the index finger of the right hand whenever they detected a target. For a response to be correct, it had to be between 100 and 800 ms after target onset. There were always at least two non-target trials between target trials, but we did not explicitly inform participants about this contingency. In fixation conditions, fixation dot increments had a duration of 100 ms with a random onset asynchrony of 50, 150, 250, 350, or 450 ms from stimulus onset. There were equal numbers of the different onset asynchronies. Participants completed all the blocks for one condition before moving onto another.

2.2.5 | Eye tracking recording and analysis

The eye-tracker monitored gaze positions of both eyes at a sampling rate of 500 Hz. We analyzed gaze position at stimulus onset for standard, deviant, and control stimuli in each condition. We excluded gaze data for the first two stimulus events in each block, for target trials, and for trials that immediately followed a target or deviant stimulus. To correct for any systematic bias of the eye-tracker, we calculated the median of gaze position in bar-fixation condition and the median of gaze position in Gabor-fixation using standard and deviant trials in oddball blocks per eye and participant. We then corrected the gaze position by the mean of these two medians in all conditions.

We averaged gaze data over eyes after excluding any trial containing a blink or a gaze position horizontally or vertically exceeding ±3° visual angle from the center at trial onset. We computed probability density maps for each condition and block type by accumulating gaze positions across trials and blocks per condition and block type normalized by the number of included trials. We filtered probability density maps by a Gaussian kernel with an *SD* of 0.25° visual angle.

2.2.6 | EEG recording and data analysis

We recorded the electroencephalogram (EEG) from 29 silver/silver chloride electrodes attached to an electrode cap (actiCAP). We placed electrodes at AF3, AF4, F3, Fz, F4, F5, F6, FC1, FC2, FC5, FC6, C3, Cz, C4, T7, T8, CP1, CP2, CP5, CP6, P3, Pz, P4, P7, P8, O1, and O2 according to the extended international 10−20 system and at the left and right earlobe. We recorded EEG at a 500 Hz sampling rate and a time constant of 10 s with a BrainAmp DC system (Brain Products, Gilching, Germany). We recorded the electrooculogram (EOG) from electrodes placed lateral to the outer canthi of both eyes and an electrode placed below the left eye.

Impedances were kept below 20 kΩ. We placed the ground electrode on the upper forehead and the reference electrode on the nose-tip (same as Kimura et al., 2009).

We completed preprocessing using MATLAB (R2015b; MathWorks Inc.), EEGLAB (14.1.1; Delorme & Makeig, 2004), and ERPLAB (6.1.4; Lopez-Calderon & Luck, 2014). We filtered the continuous EEG and EOG activity with a high-pass 0.1 Hz Kaiser-windowed (beta 5.65) sinc FIR filter (order 9,056) and low-pass 40 Hz Kaiser-windowed (beta 5.65) sinc FIR filter (order 184). Epochs were 500 ms long, including a 100 ms pre-stimulus baseline. We excluded the first two trials in each block, target trials, trials that immediately followed a target, and trials that immediately followed a deviant stimulus. We also excluded epochs including amplitude changes exceeding 800 μV at any channel to exclude non-stereotypical artifacts that are not likely to reflect eye movements or blinks that can be identified and removed later via ICA.

We identified noisy channels using the technique recommended by Bigdely-Shamlo, Mullen, Kothe, Su, and Robbins (2015). That is, we excluded EEG channels with unusually high deviations in activity (calculated as a z score exceeding 3.0 with a *SD* of 0.7413 times the interquartile range). This affected no more than three electrodes per participant in seven participants.

We corrected data for artifacts using independent component analysis (ICA) with AMICA (Delorme, Palmer, Onton, Oostenveld, & Makeig, 2012). To improve the decomposition, we computed the ICA on the raw data (excluding bad channels) filtered by a 1-Hz high-pass (Kaiser-windowed sinc FIR filter, order 804, beta 5.65) and 40 Hz low-pass filter and epoched, but not baseline corrected (Groppe, Makeig, & Kutas, 2009). We then applied the obtained de-mixing matrix to the 0.1−40 Hz filtered data. Winkler, Debener, Müller, and Tangermann (2015) have validated that high-pass filters improve ICA decompositions (reliability, independence, and dipolarity) and the de-mixing matrix can be applied to a linearly transformed data set.

We removed artifactual independent components from each participant's data by using SASICA (Chaumon, Bishop, & Busch, 2015; Makeig, Bell, Jung, & Sejnowski, 1996) to determine which exhibited low autocorrelation, low focal channel or trial activity, high correlation with vertical or horizontal EOG, or met ADJUST criteria (Mognon, Jovicich, Bruzzone, & Buiatti, 2011). We manually removed artifactual components using Chaumon et al.'s (2015) criteria, retaining those with any sign of neural activity based on consistent activity time-locked to stimulus onset, on topography, or on a 1/f-like power spectrum.

We next excluded any epochs containing amplitude changes exceeding ±100 μV at any channel. We interpolated noisy channels using spherical splines (Perrin, Pernier, Bertnard, Giard, & Echallier, 1987). We averaged ERPs separately for the standard, deviant, and control stimuli in each condition. The average number of epochs in each ERP appears in Table 2.

TABLE 2 Mean number (*SD*) of epochs per participant in the grand average ERP for each condition and trial type

Condition	Standard	Deviant	Control
Bar-edge	495 (19)	194 (6)	171 (5)
Bar-fixation	488 (28)	190 (8)	169 (8)
Gabor-edge	486 (33)	188 (15)	167 (12)
Gabor-fixation	484 (34)	188 (13)	168 (9)

We then subtracted ERPs to controls and ERPs to standards from ERPs to deviants to produce a deviant-minus-control difference wave, revealing the genuine vMMN, and a deviant-minus-standard difference wave, revealing the classic vMMN.

We conducted temporal principal component analysis (PCA) on the ERP data using the EP toolkit (v2.64; Dien, Khoe, & Mangun, 2007). The structure of exogenous components was considerably different between bar and Gabor conditions. Therefore, we conducted PCA separately for bar and Gabor conditions on the individual average ERP data in deviant and control trials. We used Promax rotation ($\kappa = 3$) with a covariance relationship matrix and Kaiser weighting. Based on Horn's (1965) parallel test, we retained 12 components, explaining more than 95% of the variance.

We replicated the statistical tests for the genuine vMMN reported by Kimura et al. (2009) for all our conditions from 200 to 250 ms at P7 and P8. As well, we conducted Bayesian t tests, and Bayes Factor replication tests (Verhagen & Wagenmakers, 2014) using posterior distributions according to the results reported by Kimura et al. (2009) as priors. For the bar-edge condition, we also conducted the same tests for the classic vMMN and for adaptation (controls minus standards) from 100 to 150 ms at (interpolated) PO7 and PO8 and from 200 to 250 ms at P7 and P8.

We also performed repeated-measures Bayesian analysis of variances (ANOVAs),[2] Bayesian paired t tests, traditional repeated-measures ANOVAs, and paired t tests on deviant-related amplitude differences in component scores at sites of

[2]The model with the largest Bayes Factor (BF_{10}) is the *favoured model*. The main effects and interactions within such a model are, therefore, important for explaining the data. The inclusion Bayes Factor ($BF_{\text{Incl.}}$) is the extent to which the data support inclusion of the factor of interest. The $BF_{\text{Incl.}}$ compares the posterior probability of matched models including versus excluding the effect or interaction. Following Lee and Wagenmakers (2013), we took as strong evidence for the alternative model if BF_{10} was larger than 10, moderate evidence if BF_{10} was between 10 and 3, and weak evidence if BF_{10} was between 3 and 0.33. We took as substantial evidence for the null model if BF_{10} was between 0.33 and 0.1, and strong evidence if the BF_{10} was less than 0.1.

PCA components' peaks (e.g., P8 and O2). We compared all models (constrained by the principle of marginality) with the null model (BF_{10}) and additionally evaluated main effects and interactions by comparing the models containing a main effect or interaction to the equivalent models stripped of the effect excluding higher order interactions ("Baws Factor" or "Inclusion Bayes Factor" based on matched models; Mathôt, 2017). All t tests were one-tailed (as used by Kimura et al., 2009) unless explicitly stated and we used medium effect size priors for all Bayesian analyses. We employed the Greenhouse–Geisser correction (ε) for degrees of freedom where appropriate. Eta squared (η^2) denotes the estimated effect size.

2.3 | Results

2.3.1 | Behavioral performance

Over both tasks, mean hit rates were 88% (SD ± 5%) and false alarm rates were 0.33% (SD ± 0.32%). To determine whether there were any differences in task performance, we performed paired, two-tailed t tests and Bayesian two-tailed t tests on hit rates and false alarm rates. Hit rates were 5% better for the edge task (90% ± 7%) than for the fixation task (85% ± 6%), $t(23) = 2.759$, $p = .011$, $BF_{10} = 4.409$; there was no difference in false alarm rates between the two tasks (0.37% ± 0.34% and 0.29% ± 0.38%), $t(23) = 1.266$, $p = .218$, $BF_{10} = 0.437$. The differences in hit rates are unlikely to have affected the ERPs because we excluded trials including targets or responses.

In our experiment, the difference between hit rates in standard and deviant trials in the bar-edge condition was −0.3% (standard trials: 92.2% ± 7.0%, deviant trials: 92.5% ± 7.0%). In Kimura et al.'s experiment, the difference was much greater at 4.2% (standard trials: 93.1% ± 6.2%, deviant trials: 88.9% ± 14.8%). The difference between false alarm rates in standard and deviant trials was −0.3% in our bar-edge condition (standard trials: 0.3% ± 0.3%, deviant trials: 0.6% ± 0.9%) and double, −0.6%, in Kimura et al.'s (standard trials: 0.1% ± 0.2%, deviant trials: 0.7% ± 0.8%).

2.3.2 | Eye movement behavior

In Figure 2, we show probability density maps for the fixation positions for all trials accumulated across all participants according to block type (oddball vs. equiprobable control), stimulus (bar vs. Gabor), and task (edge vs. fixation).

For the bar-edge oddball condition, we normalized gaze positions to one orientation. Without rotation, its probability density map looked like a fog; with rotation, gaze positions lined up along the bar, more frequent toward the bar ends. For the other conditions, it was the opposite: the probability density maps were better defined by ignoring the orientation of the stimuli.

Figure 2 shows that giving participants a central fixation task was associated with gaze around the center of the stimulus, more variable for bars than for Gabor patches. In oddball blocks, giving participants a task at the edges of the stimuli was associated with gaze toward the ends of bars and toward the upper edge of Gabor patches. In equiprobable blocks, gaze on bars was highly variable, but more frequent near the center; gaze on Gabor patches was similar to that from oddball blocks.

2.3.3 | Event-related potentials and difference waves

Figure 3 shows the ERPs and difference waves for each condition. The general form of our ERPs is typical of those recorded from the parieto-occipital regions on the scalp in other vMMN studies (e.g., File et al., 2017; Kimura & Takeda, 2015), with a P1, an N1, and a P2. We show these ERP components at the P8 electrode Gabor-fixation condition in Figure 3.

The difference waves in Figure 3 are green for deviant-minus-standards and purple for deviant-minus-controls. The figure also shows the 95% confidence intervals. The green traces show some negativities, especially from electrode P8 from the bar-edge condition; these could be classic vMMNs (i.e., contributed to by adaptation). But these negativities are smaller and briefer than those found by Kimura et al. (2009) (see also Tables S1 and S2).

Purple traces are positive for the entire vMMN time window for bars and fluctuate randomly around zero for Gabor patches, showing no genuine vMMN. This is very different from that found by Kimura et al. (2009), who did find a genuine vMMN.

We could not help noticing an early positivity of deviants relative to controls commencing about 80 ms after stimulus onset at occipital electrodes in our bar-fixation and Gabor conditions (it also is visible in the bar-edge condition but starting after P1). We explore this later.

Classic vMMN and adaptation from 100 to 150 ms and from 200 to 250 ms in the bar-edge condition (replication of Kimura et al., 2009)

From 100 to 150 ms, we found a significant, small, classic vMMN for (interpolated) PO8, $M = -0.48$ μV, $t(23) = -1.900$, $p = .035$, $BF_{-0} = 1.917$. The negativity was not significant at PO7, $M = -0.19$ μV, $t(23) = -0.825$, $p = .209$, $BF_{-0} = 0.456$. Because our effect sizes were smaller than Kimura et al.'s, the corresponding replication Bayes Factor results show strong evidence for the null model,

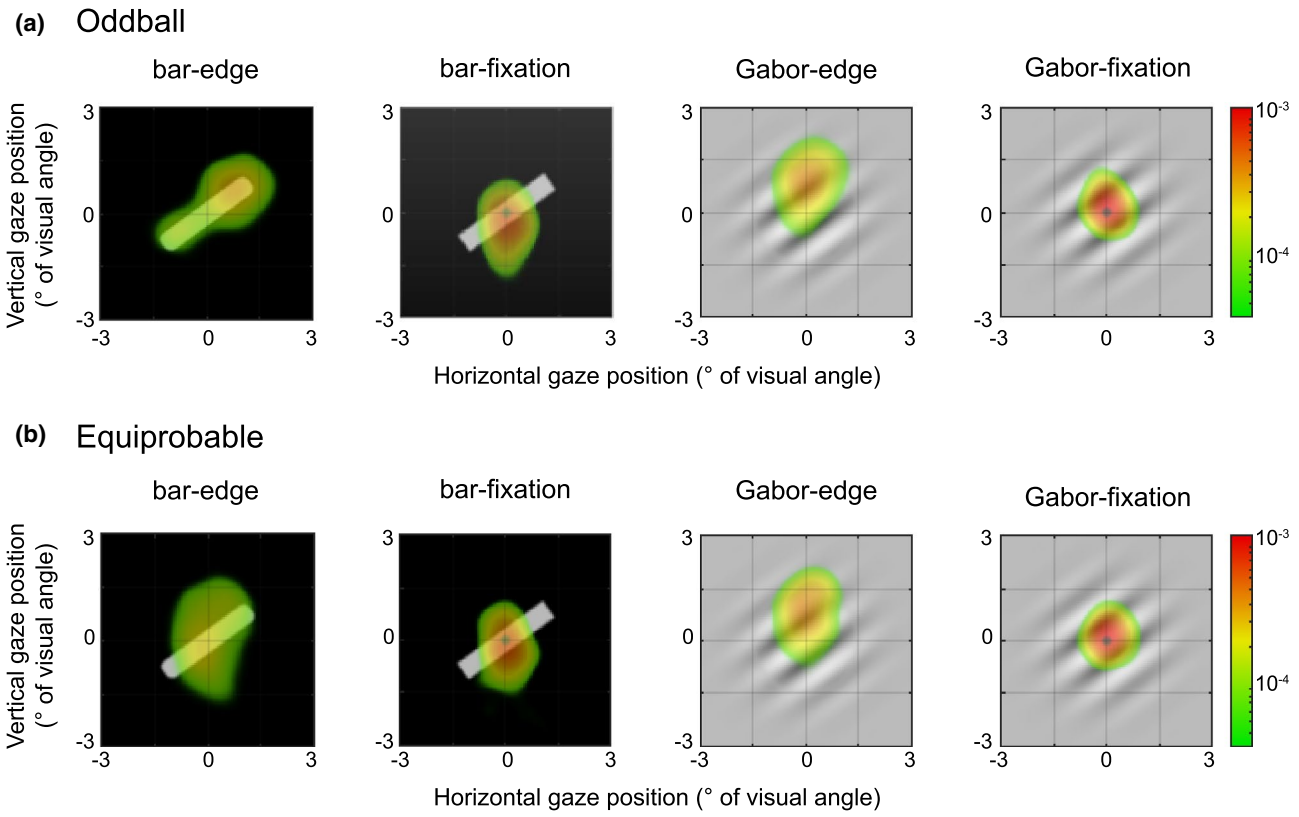

FIGURE 2 Probability density maps for aggregated gaze data from all participants in Experiment 1. Coordinates for all accepted trials from each condition are standardized relative to individual gaze position. For the bar-edge, oddball condition, coordinates are standardized to the depicted orientation. Colors reflect the probability that location was fixated at stimulus onset across trials in this condition. (a) Results from oddball trials. (b) Results from equiprobable control trials

$BF_{r0} = 0.0063$ and 0.0009, respectively. We also found adaptation effects (control minus standard) that were smaller than Kimura et al.'s; ours were not significant, either for PO7, $M = -0.31$ μV, $t(23) = -1.057$, $p = .151$ $BF_{-0} = 0.594$, $BF_{r0} = 0.0179$, or for PO8, $M = -0.30$ μV, $t(23) = -1.066$, $p = .149$, $BF_{-0} = 0.600$, $BF_{r0} = 0.0008$.

From 200 to 250 ms, we found a significant, smaller, classic vMMN for P8, $M = -0.67$ μV $t(23) = -1.741$, $p = .048$, $BF_{-0} = 1.498$, $BF_{r0} = 0.0814$. The negativity was not significant at P7, $M = -0.19$ μV, $t(23) = -0.487$, $p = .316$, $BF_{-0} = 0.324$, $BF_{r0} = 0.0034$. We found statistically significant adaptation effects at P8, $M = -1.46$ μV, $t(23) = -4.489$, $p < .001$, $BF_{-0} = 342.980$, $BF_{r0} = 897.828$, and at P7, $M = -1.18$ μV, $t(23) = -3.044$, $p = .003$, $BF_{-0} = 15.361$, $BF_{r0} = 24.299$.

Genuine vMMN from 200 to 250 ms in the bar-edge condition (replication of Kimura et al., 2009)

In the bar-edge task condition, we found no genuine vMMN from 200 to 250 ms at P7 or P8 electrode location, as reported by Kimura et al., but instead a small positive difference potential. Given the very large effect size reported by Kimura et al., the data provide strong evidence for the null hypothesis in Bayes Factor replication tests, $BF_{r0} = 0.0031$ and 0.0005, respectively. The data also provide strong evidence for the null hypothesis in directed Bayesian t tests, $M = 0.99$ and 0.79 μV, $t(23) = 3.027$ and 2.324, $p = .997$ and .985, $BF_{-0} = 0.063$ and 0.074, respectively.

Genuine vMMN in the bar-fixation condition

For this and the remaining conditions, we searched only for the genuine vMMN from 200 to 250 ms. In the bar-fixation condition, we found no genuine vMMN from P7 or P8. The data provide strong evidence for the null hypothesis in Bayes Factor replication tests, $BF_{r0} = 0.002$ and 0.0005, and in directed Bayesian t tests, one-tailed, $M = 0.39$ and 0.62 μV, $t(23) = 1.567$ and 2.293, $p = .935$ and .984, $BF_{-0} = 0.093$ and 0.074.

Genuine vMMN in Gabor-edge condition

In the Gabor-edge condition, we again found no significant genuine vMMN from P7 or P8 from 200 to 250 ms. The data provide strong evidence for the null hypothesis in Bayes Factor replication tests, $BF_{r0} = 0.110$ and 0.003, but do not provide conclusive evidence in directed Bayesian t tests, one-tailed, $M = -0.20$ and -0.13 μV, $t(23) = -1.575$ and -0.625, $p = .065$ and .269, $BF_{-0} = 1.171$ and 0.370.

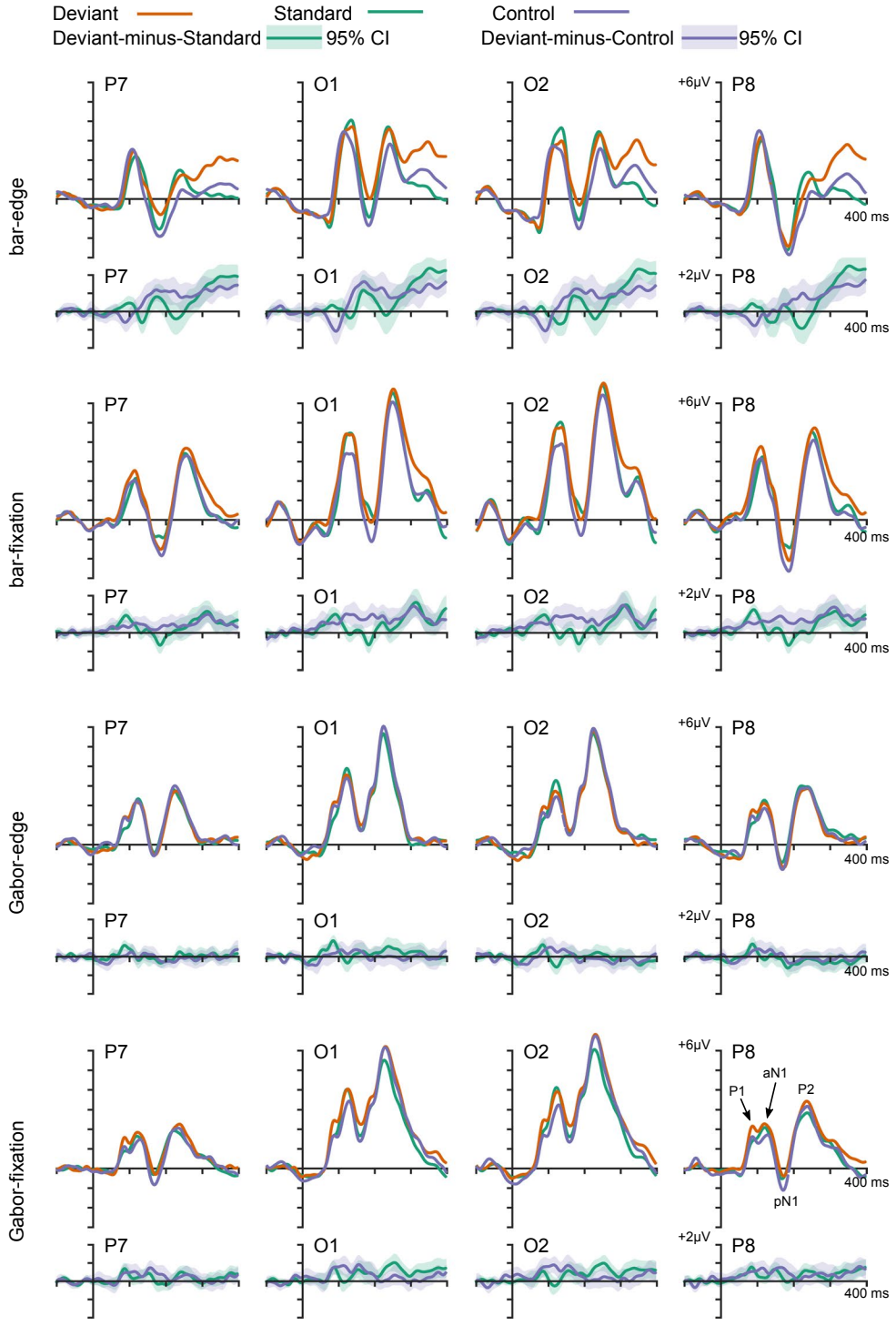

FIGURE 3 ERPs and difference waves from P7, O1, O2, and P8 electrodes from Experiment 1. We illustrate the P1, positive pole of the anterior N1 (aN1), posterior N1 (pN1), and P2 at P8 electrode, Gabor-fixation condition

Genuine vMMN in the Gabor-fixation condition

In the Gabor-fixation condition, we also found no genuine vMMN from P7 or P8 from 200 to 250 ms. Instead, there was a small, positive, deviant-minus-control difference potential. The data provide strong evidence for the null hypothesis in Bayes Factor replication tests, $BF_{r0} = 0.002$ and 0.0005, and substantial evidence for the null hypothesis in directed Bayesian t tests, one-tailed, $M = 0.15$ and 0.18 μV, $t(23) = 0.751$ and 0.790, $p = .770$ and .781, $BF_{-0} = 0.133$ and 0.130.

Outside the vMMN time window

Outside of 100–300 ms, we did not observe any relevant negative deflections of the deviant-minus-control ERP difference wave exceeding the 95% confidence interval; except

in the bar-edge condition. In it, we observed a very small early negativity, prior to 100 ms, a small early positivity, after 100 ms, and a large late positivity, after 300 ms. We analyze the early positivity next; we do not further analyze the late positivity, except to say it may be a P3b because deviants reminded participants to keep their eyes on the center of the bar.

2.3.4 | Principal component analysis of event-related potentials

To detect any potential genuine vMMN PCA component, we computed ANOVAs for all components with a peak latency between 100 and 300 ms and a negative deviant-minus-control difference score in at least one condition or task at the peak electrode location—usually parietal or occipital. We did not find any significant main effect of stimulus type or interaction effect including stimulus type (all $BF_{10} < 0.5$; except for P1 in the bar conditions; see below). Although we did not identify any component that was temporally or spatially characteristic of the vMMN, we did find some PCA components sensitive to deviants, some earlier than 100 ms.

P1 and N1 components

PCA of the data confirmed early differences in amplitude seen in our ERPs (80−200 ms in Figure 3). Figure 4 shows that the temporal and topographical profiles of the P1 and N1 components were different between bar and Gabor conditions. In the bar conditions, the P1 component had a peak latency of 110 ms (maximal over lateral parietal electrodes). An anterior N1 component with a peak latency of 146 ms (minimal over fronto-central electrodes and maximal over occipital electrodes) and a posterior N1 component with a peak latency of 200 ms (minimal over lateral parietal electrodes and maximal over fronto-central electrodes) followed.

In the Gabor conditions, the P1 peak latency was 86 ms (maximal over occipital electrodes), an anterior N1 component with a peak latency of 126 ms (minimal over fronto-central electrodes and maximal over occipital electrodes), and a posterior N1 component with a peak latency of 170 ms (minimal over lateral parietal and maximal over occipital electrodes) followed.

P1. In the bar conditions, we found an interaction between task and stimulus type, $F(1, 23) = 9.339$, $p = .006$, $\eta^2 = 0.289$, $BF_{\text{Incl}} = 1.641$. Paired tests revealed not-significantly smaller P1 (PCA component 5) amplitudes for deviants than for controls in the edge task, $t(23) = -1.808$, $p = .084$, $BF_{10} = 0.872$, but significantly larger P1 amplitudes for deviants than controls in the fixation task, $t(23) = 2.781$, $p = .011$, $BF_{10} = 4.600$ (see Figure 4 top panel, left).

In the Gabor conditions, P1 (PCA component 7) amplitudes were larger for deviants than controls, however, the data do not provide conclusive evidence for the favored model including the stimulus type main effect, $F(1, 23) = 4.463$, $p = .046$, $\eta^2 = 0.163$, $BF_{10} = 1.332$ (see Figure 4 top panel, right).

Anterior N1. In the bar conditions, at occipital electrodes, the anterior N1 (PCA component 3, shown as aN1 in Figure 3) amplitude was more positive in the fixation task than in the edge task, $F(1, 23) = 10.984$, $p = .003$, $\eta^2 = 0.323$. Amplitudes were also more positive for deviants than for controls, $F(1, 23) = 11.576$, $p = .002$, $\eta^2 = 0.335$ (see Figure 4, middle panel, left). The data provide strong evidence for the favored model including both main effects ($BF_{10} = 2{,}619.138$) as well as substantial evidence against a moderation of the stimulus type effect by the task ($BF_{\text{Incl}} = 0.319$).

Also, in the Gabor conditions, at occipital electrodes, the anterior N1 (PCA component 3) amplitudes were more positive in the fixation task than in the edge task, $F(1, 23) = 8.281$, $p = .009$, $\eta^2 = 0.265$, and for deviants than for controls, $F(1, 23) = 16.834$, $p < .001$, $\eta^2 = 0.423$ (see Figure 4, middle panel, right). The data provide strong evidence for the favored model including both main effects ($BF_{10} = 537.932$) as well as substantial evidence against a moderation of the stimulus type effect by the task ($BF_{\text{Incl}} = 0.345$).

In short, the data show that the stimulus type (i.e., deviant vs. control) determines anterior N1 positivity at occipital electrodes—deviants produce larger positivities than controls—and this occurs for bar and Gabor stimuli regardless of the task.

Posterior N1. In the bar conditions, the posterior N1 (PCA component 2) amplitude was more positive in the fixation task than in the edge task, $F(1, 23) = 6.189$, $p = .021$, $\eta^2 = 0.212$, and more positive for deviants than for controls, $F(1, 23) = 6.947$, $p = .015$, $\eta^2 = 0.232$ (see Figure 4, bottom panel, left). The data provide strong evidence for the favored model including both main effects ($BF_{10} = 36.845$) as well as substantial evidence against a moderation of the stimulus type effect by the task ($BF_{\text{Incl}} = 0.282$).

In the Gabor conditions, we observed an interaction of stimulus type and task on the posterior N1 (PCA component 4) in the frequentist statistics, $F(1, 23) = 7.968$, $p = .010$, $\eta^2 = 0.257$. However, the Bayes factor analysis is inconclusive and rather provides weak evidence against the interaction ($BF_{\text{Incl}} = 0.525$). The N1 amplitude was more positive for deviants compared to controls in the fixation task, $t(23) = 2.593$, $p = .016$, $BF_{10} = 3.226$, but there was no difference between deviants and controls in the edge task, $t(23) = 0.124$, $p = .903$, $BF_{10} = 0.216$ (see Figure 4, bottom panel, right). Further, the data do not provide conclusive evidence for any of the models (all $BF_{10} < 0.5$).

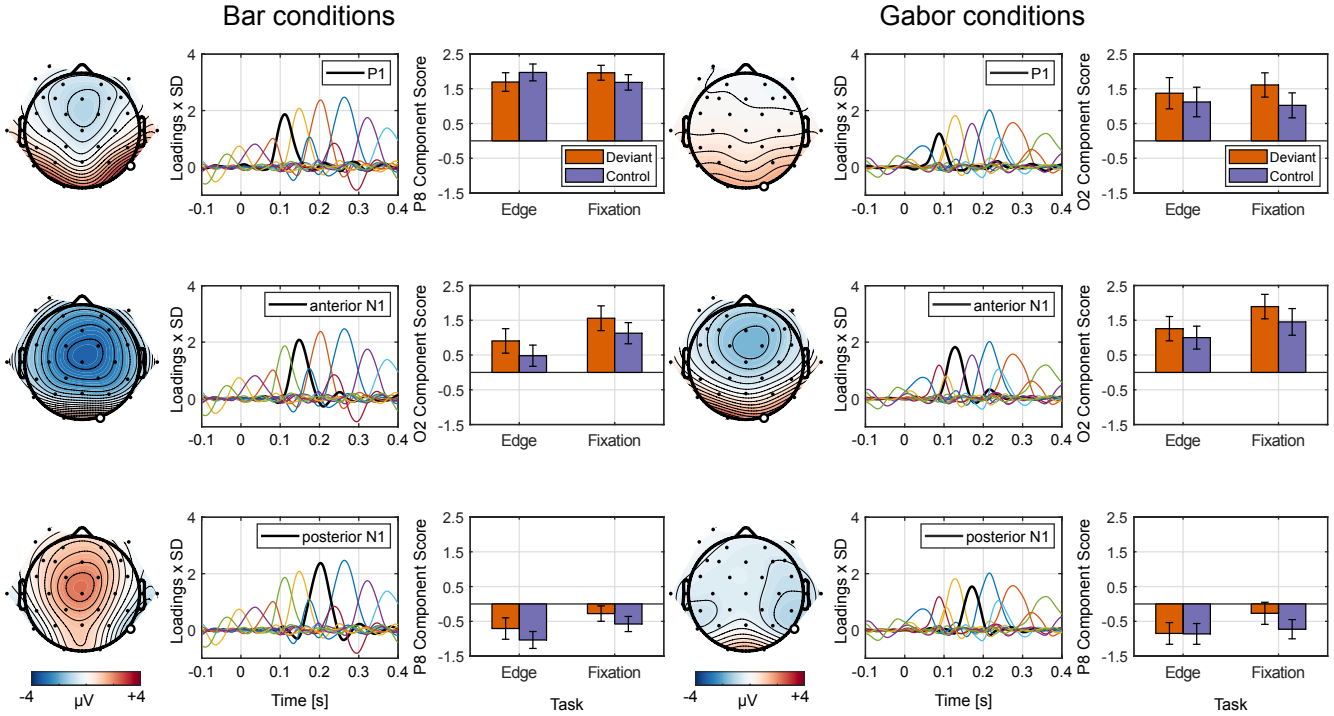

FIGURE 4 Principal components contributing to early increased positivity in deviant-minus-control difference wave for bar and Gabor conditions in Experiment 1. The top row shows details of the P1 in the bar (left three panels) and Gabor (right three panels) conditions. The middle row shows details of the anterior N1 in the same conditions. The bottom row shows details of the posterior N1. Columns 1 and 4 show topographical maps of the average activity from deviant and control trials at peak latency. Columns 2 and 5 show component loadings (scaled by *SD*) against the time course of each component's contribution (thick black line) to the overall evoked activity recorded from the scalp relative to all other components (thin multi-colored lines). Columns 3 and 6 show component scores for deviant and control trials in each stimulus and task condition at the electrode illustrated on the corresponding topographical map. Error bars depict ± 1 *SE*.

2.4 | Discussion

We could not find any convincing evidence of a genuine vMMN in any condition. This is particularly surprising because we replicated Kimura et al.'s (2009) stimuli and procedure in our bar-edge condition. We consider possible reasons next. Then, we consider implications of the absence of a genuine vMMN in any condition.

2.4.1 | Replication of Kimura et al. (2009)

There were four major differences in the method of the two studies:

1. We monitored eye positions, whereas Kimura et al. did not. We found that when participants' task was in the center of stimuli, they looked there. When their task was at the edge of the stimuli, they looked slightly up and slightly to the right of center, except for bars in oddball blocks, in which they looked toward the end of the bars.

In the bar-edge condition for oddball blocks, looking toward a bar's end would help target detection, whereas in the control blocks, it would not. In the control blocks the orientation of the bars changed on every trial, so if participants moved their eyes, they would have been fruitlessly pursuing the location of the task-relevant information, always one trial behind. In fact, they looked toward the center.

It was the same in the Gabor-edge condition. In both sorts of blocks, the information was in a ring at the edge, so participants could have looked in any direction toward the edge to do the task. We suspect their slight tendency to look up and to the right of center reflects the principles found when people look at arbitrary images—that they are highly variable, but generally aimed at areas of salience (e.g., Quiroga & Pedreira, 2011) and they follow the normal pattern of scanning eye movements from reading (e.g., Spence, 2019).

If our participants, who knew we were monitoring their gaze, looked strategically at different parts of the stimuli depending on the task, then, it is quite possible that Kimura et al.'s participants, whose eye positions were not monitored, looked even more strategically than ours did, at the bar ends.

2. We had other fixation (and stimulus) conditions, whereas Kimura et al. did not. Our fixation conditions gave our participants practice at fixating centrally. This may well have transferred to our edge conditions, leading to more accurate central fixation than in Kimura et al.'s participants.

Consider the stimuli during the oddball block for Kimura et al.'s participants if they consistently looked at the bar ends. During the standard trials, a grey bar end filled the fovea. During deviant trials, the black background filled the fovea. This turns an orientation deviant into a large decrement in luminance for the fovea. About 50% of the area of the visual cortex is devoted to processing input from the fovea covering only 1% of the retinal size (Kolb, Fernandez, & Nelson, 2018), which will, therefore, have a much greater influence on ERPs than any similar area of the rest of the retina. This combined change in orientation and luminance may be sufficient for yielding the vMMN, whereas a change in orientation alone is not.

Possibly our participants did not show much evidence of genuine vMMNs because they fixated more centrally on more trials than Kimura et al.'s did. Our observation of considerable differences between hit and false alarm rates in standard and deviant trials in the bar-edge condition in our experiment compared to that by Kimura et al. (2009) supports our interpretation of differences in fixation behavior. With increasing gaze eccentricity along the bar, the hit rate should increase in standard trials due to higher discriminability as the bar end moves toward the fovea but to decrease for deviant trials and vice versa for the false alarm rate. This is the pattern we observe in the data. The remarkably high inter-individual variability of the hit rate in deviant trials in Kimura et al.'s study might indicate that participants' fixation behavior followed different strategies.

3. We had fewer control trials than Kimura et al. We do not expect our lower number of control trials than Kimura et al.'s (2009) affected the vMMN measurement because signal-to-noise ratio in the difference wave is limited by the condition with fewest trials. In Kimura et al. (2009) this is the deviant condition. The number of trials in our deviant ERP (maximum 200 trials) is about 67% of theirs. Moreover, we had twice as many participants than Kimura et al., leading to very good signal-to-noise ratio across all conditions (see 95% confidence intervals in Figure 3). The Bayesian replication tests clearly support the notion that the absence of a vMMN was not due to lack of power or noise in the data. Furthermore, we were able to detect deviant-related differences in other components: the P1, anterior N1, and posterior N1.

4. We used different preprocessing of the data from Kimura et al. To check whether our failure to replicate the results of Kimura et al. (2009) was because our preprocessing of our EEG data differed from theirs, we used their preprocessing steps for our data. We give the details in the Supplementary Materials (Figure S1 and Tables S1 and S2). Nothing we found in the new analyses altered our characterization of our results: we found a small, classic vMMN between 200 and 250 ms and no evidence of a genuine vMMN.

2.4.2 | Implications of the absence of a genuine vMMN in any condition

We hope we have shown that the differences in methodology we raised in points 3 and 4 were not responsible for the differences between our results and those of Kimura et al. (2009). It is possible that the differences we considered in points 1 and 2, in gaze position, were responsible.

Other studies of the orientation vMMN with bars might have involved a similar lack of control of gaze position, possibly explaining why some have found the vMMN using bar stimuli, whereas others have not. For example, Astikainen et al. (2008), who did find a genuine vMMN to bars, had their participants attend to auditory stimuli, allowing their fixation to stray away from the center of the bars. In contrast, File et al. (2017), who did not find a vMMN, used a demanding fixation task, ensuring that their oriented bars always fell on the same retinal locations.

The absence of a genuine vMMN in our conditions requiring central fixation, diverting attention from the oriented stimuli, is consistent with recent studies (e.g., File et al., 2017; Smout, Tang, Garrido, & Mattingley, 2019). Indeed, various authors have questioned whether the auditory MMN is preattentive (e.g., Auksztulewicz & Friston, 2015; Sussman, Chen, Sussman-Fort, & Dinces, 2014; Woldorff, Hackley, & Hillyard, 1991; Woldorff & Hillyard, 1990).

We found that, except for the bar-edge condition, P1 amplitudes are larger for deviants than for controls. Perhaps the larger variance in gaze position (cf. Figure 2) disguised the true effect of deviants on P1 amplitudes. Of course, the variance in our post hoc analyses of P1 amplitudes could be due to other factors we have not considered.

We also found that, according to our Bayesian and frequentist analyses, the positive pole of the anterior N1 is larger for deviants than controls and this is consistent across all conditions, suggesting it may be a reliable marker for deviance-related activity.

Another possibility is that we failed to find the vMMN from differences in precursory stimulus processing, as evidenced by differences in early deviant-related activity or the absence of adaptation effects that Kimura et al. reported for controls versus standards between 100 and 150 ms. Therefore, to conclude with greater certainty that our results were truly reflective of changes in low-level properties of visual stimuli, we conducted a second experiment.

3 | EXPERIMENT 2

3.1 | Introduction

In addition to testing, again, whether orientation differences of 36° yield a genuine vMMN, we also wanted to examine whether changes in other properly isolated low-level visual

features could yield genuine vMMNs. We searched for genuine vMMNs for changes in orientation, Michelson contrast, phase, and spatial frequency. We carefully manipulated each low-level feature of visual input without affecting other features using Gabor patches. We compared ERPs to standards and deviants from multi-feature blocks and ERPs to control deviants from cascadic-control blocks (Ruhnau et al., 2012).

3.2 | Method

Some aspects of the method of Experiment 2 were identical to those of Experiment 1, including the number of participants, inclusion criteria, the EEG apparatus, most properties of the Gabor patches, all properties of the fixation dots, the central fixation task, the EEG-recording, EEG preprocessing, and statistical analysis of the ERP data. The mean age of our 24 new participants was 23.13 years with a range of 18–38 years (9 males, 23 right-handed). The method differed in that we used a multi-feature paradigm, a cascadic-control condition, and we did not measure participants' gaze positions. We also included posttest blocks to assess the discriminability of each deviant stimulus feature, avoiding issues associated with feature changes that are near the discrimination threshold (as shown by Horváth et al., 2008, for auditory input).

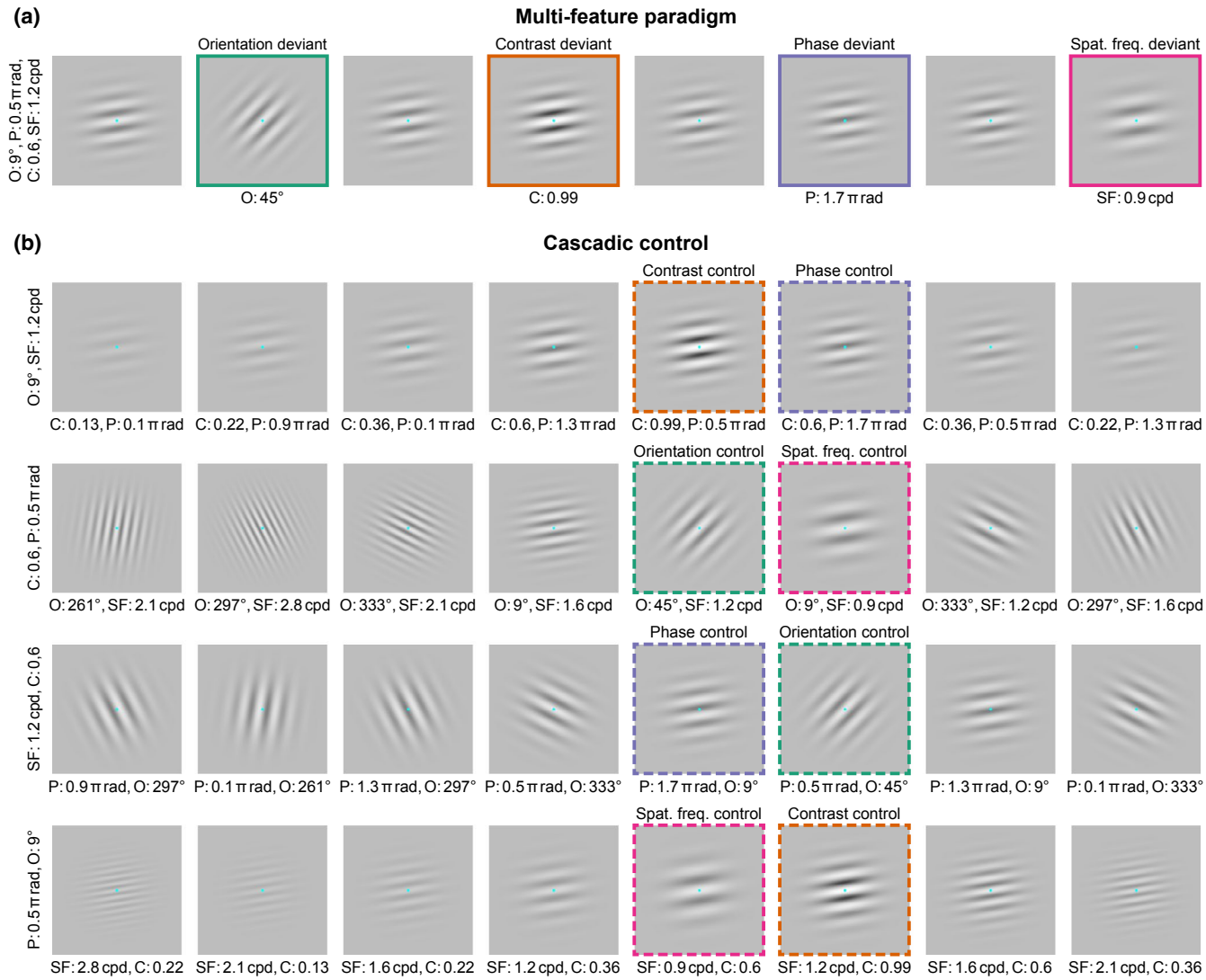

FIGURE 5 Illustration of the stimuli and procedure of Experiment 2. (a) Example of eight trials of a multi-feature block. The first panel shows the standard. The next panel, outlined in green, shows an orientation deviant (36° orientation difference from the standard). The next deviant panel, outlined in orange, shows a contrast deviant (0.33 greater than the standard). The next deviant panel, outlined in violet, shows a phase deviant (1.2π radians difference from the standard). The final deviant panel, outlined in magenta, shows a spatial frequency deviant (33% less than the standard). (b) Examples of eight trials of four kinds of cascadic-control blocks. The top row shows stimuli that change regularly in contrast and phase from trial to trial. The control stimuli for contrast and phase—physically identical to the deviants from the multi-feature blocks—are outlined in dashed orange and dashed violet. The remaining rows of panels show other combinations of stimulus features with stimuli that serve as controls for other deviants. The color scheme is the same as in (a). For each control stimulus, we show its relevant orientation (O; °), Michelson contrast (C), phase (P; radians), or spatial frequency (SF; cpd)

3.2.1 | Stimuli

We manipulated the orientation, contrast, phase, and spatial frequency of the Gabor patches. In the multi-feature paradigm, standard Gabor patches had an orientation of 9° anticlockwise from horizontal, a Michelson contrast of 0.6, a phase of 0.5π radians, and a spatial frequency of 1.2 cpd of visual angle. Deviant stimuli had an orientation of 45° anticlockwise, or a Michelson contrast of 0.99, or a phase of 1.7π radians, or a spatial frequency of 0.9 cpd, but were identical to standard stimuli in all other features (see Figure 5a).

In the cascadic control, Gabor patches had an orientation of 45°, 9°, 333° (= 153°), 297° (= 117°), or 261° (= 81°) from horizontal (changing by 36° per trial), a Michelson contrast of 0.99, 0.6, 0.36, 0.22, or 0.13 (changing by 40% per trial), a phase of 1.7π, 0.5π, 1.3π, 0.1π, or 0.9π radians (changing by 1.2π radians per trial), and a spatial frequency of 0.9, 1.2, 1.6, 2.1, or 2.8 cpd visual angle (changing by 33% per trial).

3.2.2 | Procedure

The experiment started with written instruction and consisted of eight multi-feature blocks and eight cascadic-control blocks. We randomized block order. In the multi-feature blocks, standard and deviant stimuli appeared predictably on alternate trials (Figure 5a). Each deviant feature appeared once per set of four standard/deviant pairs of trials in pseudo-randomized order with the constraint that the same deviant feature never appeared in two subsequent pairs of trials. The probability that each deviant feature occurred in a deviant trial was 25%. Hence, for each set of eight stimuli, for each visual feature, the deviant feature was presented in one out of eight trials (12.5%) and the standard feature in seven out of eight trials (87.5%; similar to the regular oddball paradigm; see below). In each of the multi-feature blocks, there were 128 standards and 128 deviants resulting in 256 deviants per visual feature.

In the cascadic-control blocks (illustrated in Figure 5b), we interspersed physically identical standard and control stimuli within a block, in which the deviant stimulus feature was varied in a regular ascending and descending block (e.g., 1–2–3–4–5–4–3–2–1). We combined two features per block (contrast and phase, orientation and spatial frequency, phase and orientation, contrast and spatial frequency—see Figure 5b). We did not combine phase and spatial frequency because both features would interact, obscuring regularity, and we did not combine contrast and orientation for a balanced design. The two-feature cascades had an offset of one trial: each feature led once in one of two blocks, resulting in eight cascadic-control blocks. This design allowed the corresponding multi-feature standard feature to precede each control stimulus. In each of the cascadic-control blocks, there were 256 stimuli including 32 control stimuli per feature resulting in 128 control stimuli per visual feature.

In a two-interval, two-alternative, forced choice task, we asked participants to look at the Gabor patches and to judge whether two successively presented Gabor patches were the same or different. Each Gabor patch was presented for 100 ms separated by an ISI of 400 ms. The fixation dot was always present. The next trial started 400 ms after the response. There were 128 pairs per block, 64 pairs were the same (both standard Gabor patches from the multi-feature paradigm), and 64 pairs were different (16 per deviant feature from the multi-feature paradigm balanced between first and second interval). Participants responded by pressing a *same* button with the index finger of one hand and a *different* button with the index finger of other hand (counterbalanced across participants).

There was no reaction time limit for this task; however, we considered responses only between 0.1 and 2 s to remove instances in which participants took an impromptu break between trials. This resulted in a mean loss of about 2 trials in 19 participants (ranging from one to eight trials) and none in the other five participants.

3.2.3 | EEG recording and data analysis

In Table 3, we give the average number of epochs in each ERP for 24 participants. We performed PCA on the individual average ERP data in deviant and control trials. We retained 14 components (explaining more than 95% of the variance) based on Horn's (1965) parallel test.

3.3 | Results

3.3.1 | Behavioral performance

Performance on the fixation task for multi-feature (*hit rate:* 93% ± 6%, *false alarm rate:* 0.75% ± 0.65%) and cascadic

TABLE 3 Mean number (*SD*) of epochs per participant in the grand average ERP for each deviant feature and trial type. The mean number (SD) of epochs for standards was 784 (26)

Condition	Deviant	Control
Orientation	196 (7)	88 (11)
Contrast	197 (9)	88 (9)
Phase	195 (8)	88 (9)
Spatial frequency	197 (10)	88 (10)

blocks (*hit rate:* 93% ± 6%, *false alarm rate:* 0.71% ± 0.58%) was very similar: for hit rate, $t(23) = -0.598$, $p = .556$, $BF_{10} = 0.253$; for false alarm rate, $t(23) = 0.598$, $p = .556$, $BF_{10} = 0.253$). Hit rates were high (93%) and false alarm rates were low (0.73%), showing that participants devoted themselves to the task.

To derive a d-prime (d′) for each deviant feature in our discriminability blocks, we log-linear corrected (Stanislaw & Todorov, 1999). Sensitivity was worst (but still good) for phase (d′ = 2.5 ± 0.9 *SD*), better and about equal for contrast (d′ = 2.8 ± 0.8) and spatial frequency (d′ = 2.8 ± 0.7), and best for orientation (d′ = 3.5 ± 0.7), $F(3, 69) = 23.913$, $p < .001$, $\varepsilon = 0.929$, $\eta^2 = 0.510$, $BF_{10} = 7.567 \times 10^7$. All paired comparisons, aside for contrast versus spatial frequency, $t(23) = 2.781$, $p = .854$, $BF_{10} = 0.218$, were significant. Overall performance accuracy (d′ = 2.8) suggests participants were able to detect deviants with high accuracy.

3.3.2 | Event-related potentials and difference waves

Figure 6 shows the ERPs and deviant-minus-control difference waves (genuine vMMNs) for each feature deviant. ERPs and their constituents to orientation conditions are similar to those of Experiment 1 (top panel). The ERPs to the other conditions are similar to those for orientation and to ERPs reported by others. We highlight the same ERP components at P8 in the orientation condition; these are the most similar across experiments.

vMMN

We did not find a genuine vMMN in the 200–250 ms time window (as in Kimura et al., 2009) in any of the four deviant feature conditions. Table 4 shows that the data provide very strong evidence for the null hypothesis. Instead, Figure 6 shows a positive deviant-minus-control mean difference potential in the vMMN time window at electrodes P7 and P8 for all four deviant feature conditions.

Principal component analysis of event-related potentials

vMMN time window. To detect any potential vMMN PCA component, we computed ANOVAs for all components with a peak latency between 100 and 300 ms and a negative deviant minus control difference score for at least one deviant feature at the occipito-parietal component peak electrode. We found a significant interaction between stimulus type and deviant feature in two components, but all follow-up tests were not significant (all $BF_{10} < 0.5$). We did not find any significant main effect of *stimulus type* or interaction effect including *stimulus type* in any other component (all $BF_{10} < 0.5$). That is, we did not find any PCA component corresponding to the vMMN.

Although we did not find any genuine vMMN, we did observe increased early positivity to deviants compared with controls. Our PCA confirmed that this positivity was due to three separate components, as in Experiment 1.

P1 and N1 components

The components' structure and topography were highly similar to the ones observed in the Gabor conditions of Experiment 1. The peak latencies of P1 (94 ms), anterior N1 (132), and posterior N1 components (182 ms) were minimally later than in Experiment 1 (Figure 7).

P1. The P1 (PCA component 6) amplitude was more positive for deviants than for controls, $F(1, 23) = 15.209$, $p < .001$, $\eta^2 = 0.398$, but the effect was modulated by an interaction with deviant feature, $F(3, 69) = 3.782$, $p = .028$, $\varepsilon = 0.693$, $\eta^2 = 0.141$ (see Figure 7, top panel). All features, except for phase, produced a significant positive deviant minus control difference score (Table 5). However, the data provide very strong evidence for the favored model including the main effect of stimulus types and deviant feature, $F(1, 23) = 2.831$, $p = .045$, $\eta^2 = 0.110$, $BF_{\text{Incl}} = 2.291$ ($BF_{10} = 288.813$). The data provide inconclusive evidence against including the interaction between stimulus type and deviant feature ($BF_{\text{Incl}} = 0.807$).

Anterior N1. The anterior N1 (PCA component 2) amplitude at occipital electrodes was more positive for deviants than controls, $F(1, 23) = 33.139$, $p < .001$, $\eta^2 = 0.590$ (see Figure 7, middle panel). Similar to the P1, this main effect interacted with deviant feature, $F(3, 69) = 4.745$, $p = .007$, $\varepsilon = 0.884$, $\eta^2 = 0.171$. That is, all features, except for phase, produced a significant positive deviant minus control difference score (Table 4). The Bayesian ANOVA favored the model including both main effects and the interaction ($BF_{10} = 955{,}559.701$). The data provide very strong evidence for an effect of stimulus type ($BF_{\text{Incl}} = 457{,}240.641$), but only some evidence for including effects of deviant feature ($BF_{\text{Incl}} = 2.095$) and the interaction effect ($BF_{\text{Incl}} = 1.546$).

Posterior N1. The posterior N1 (PCA component 4) amplitude was more positive for deviants than for controls, $F(1, 23) = 22.623$, $p < .001$, $\eta^2 = 0.496$, and significantly different among deviant features, $F(3, 69) = 3.818$, $p = .024$, $\varepsilon = 0.757$, $\eta^2 = 0.142$. The stimulus type effect was significantly modulated by deviant feature, $F(3, 69) = 3.501$, $p = .031$, $\varepsilon = 0.773$, $\eta^2 = 0.132$ (see Figure 7, bottom panel). That is, the posterior N1 amplitude was more positive for deviants than for controls for contrast, and spatial frequency deviants, but not for orientation or phase deviants (Table 5). The Bayesian ANOVA favored the model including both main effects and the interaction ($BF_{10} = 2{,}332.248$). The data also provide very strong evidence for including deviant feature

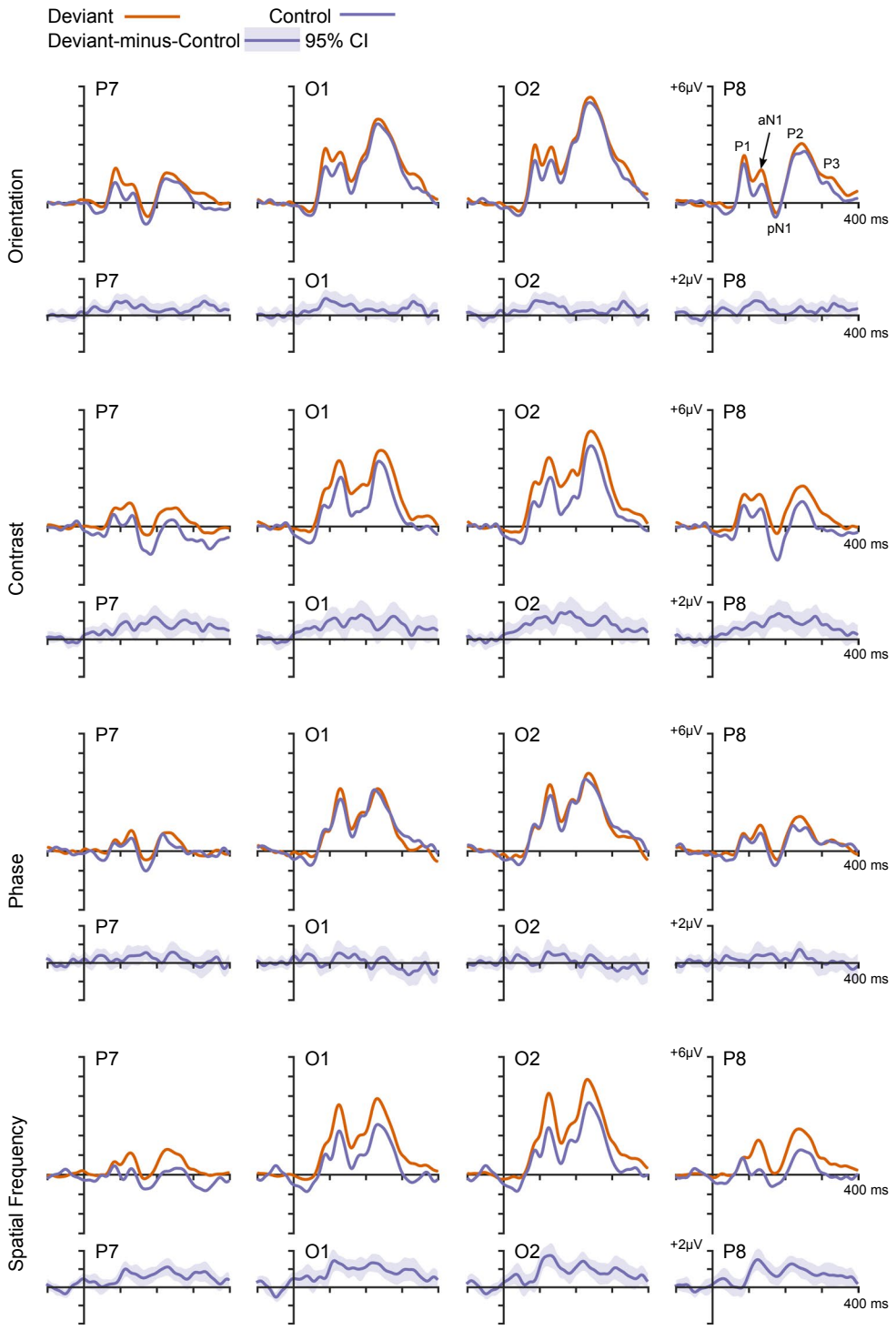

FIGURE 6 ERPs and difference waves from P7, O1, O2, and P8 electrodes from Experiment 2. We did not observe any relevant negative deflections of the deviant-minus-control ERP difference wave exceeding the 95% confidence interval (but only positive)

($BF_{\text{Incl}} = 403.809$), moderate evidence for including stimulus type ($BF_{\text{Incl}} = 3.021$), and some evidence for including the interaction effect ($BF_{\text{Incl}} = 2.583$).

Using the effect sizes for the deviant versus control Gabor-fixation stimuli at O2 (for P1 and aN1) and P8 (for pN1) in Experiment 1, we performed Bayes Factor replication tests comparing deviant and control orientation stimuli. The data provide strong evidence for the alternative for the P1 (O2: $BF_{\text{r0}} = 69.019$) and aN1 (O2: $BF_{\text{r0}} = 17.718$), but not the pN1 (P8: $BF_{\text{r0}} = 0.385$).

TABLE 4 Directed Bayesian (BF_{-0}) *t* tests (one-tailed) of mean amplitudes (μV) between 200 and 250 ms at P7 and P8 electrodes for each deviant feature ($df = 23$)

	Electrode							
	P7				P8			
Condition	μV	*t*	*p*	BF_{-0}	μV	*t*	*p*	BF_{-0}
Orientation	0.28	1.554	.933	0.093	0.25	1.199	.879	0.107
Contrast	0.78	3.133	.998	0.062	1.00	3.595	.999	0.058
Phase	0.30	1.409	.914	0.099	0.41	2.295	.984	0.074
Spatial frequency	0.98	4.988	.999	0.049	1.16	5.905	.999	0.046

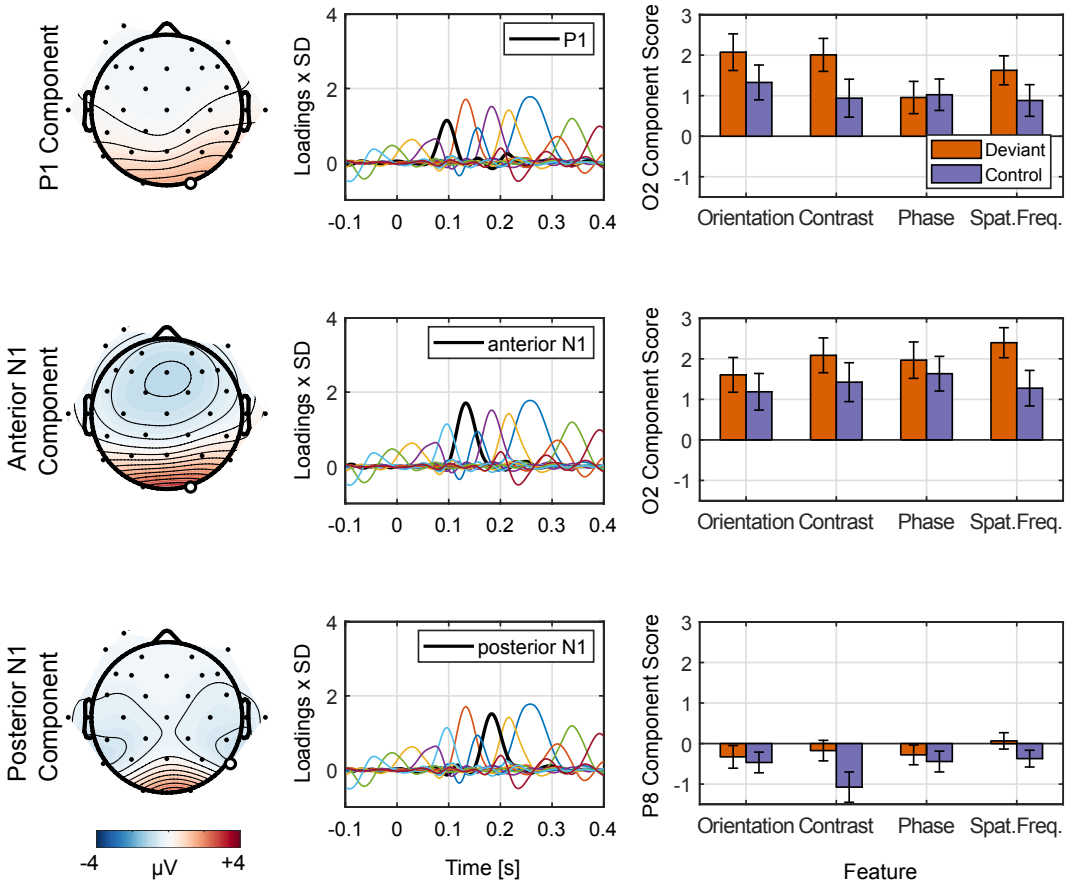

FIGURE 7 Principal components contributing to early increased positivity in deviant-minus-control difference waves in Experiment 2. The top panel shows details of the P1. The middle panel shows details of the anterior N1. The bottom panel shows details of the posterior N1. The leftmost column shows topographical maps of combined activity from deviant and control trials at peak latency. The middle column shows component loadings reflecting each component's contribution (thick black line) to the overall evoked activity recorded from the scalp relative to all other components (thin lines of different colors). The rightmost column shows bar graphs of component scores for deviant and control trials for each deviant feature at the electrode illustrated on the corresponding topographical map. Error bars depict ± 1 *SE*

3.4 | Discussion

Our Bayes Factor tests provide strong evidence of no genuine vMMN in Experiment 2. This confirms our finding from Experiment 1 that orientation deviants do not yield a vMMN when using physiologically plausible visual stimuli and controlling for adaptation and allocation of attention. Our findings also suggest that deviants in contrast, phase, and spatial frequency do not yield the vMMN.

One possibility we can discount is that the physical difference between feature levels of deviants and standards we used was too small. Except for phase, the differences we used are all many times greater than the respective discrimination thresholds: at least several tens of times for orientation (Regan & Price, 1986), and 5 to 10 times for contrast (Snowden & Hammett, 1998) and for spatial frequency (Webster, De Valois, & Switkes, 1990). We discuss phase below.

TABLE 5 Interactions with deviant feature examined with paired sample and Bayesian (BF_{10}) *t* tests (two-tailed) for the P1, anterior N1 (aN1), and posterior N1 (pN1) ($df = 23$)

Deviant feature	Electrode	*t*	*p*	BF_{10}
P1				
Orientation	O2	3.378	.003	15.313
Contrast	O2	3.411	.002	16.394
Phase	O2	−0.345	.733	0.227
Spatial frequency	O2	2.328	.029	2.005
aN1				
Orientation	O2	2.720	.012	4.095
Contrast	O2	3.527	.002	20.967
Phase	O2	1.839	.079	0.913
Spatial frequency	O2	5.908	<.001	4,040.549
pN1				
Orientation	P8	0.704	.489	0.269
Contrast	P8	3.820	<.001	39.248
Phase	P8	1.198	.243	0.406
Spatial frequency	P8	2.824	.010	5.002

It is possible that the sensitivity of the vMMN mechanism is less than when attention is devoted to the stimuli. For example, Czigler, Balázs, and Winkler (2002) showed no genuine or classic vMMN to deviants clearly differing from standards in color and luminance when attention was on a task at fixation. Smout et al. (2019) failed to show a genuine orientation vMMN when participants attended to a fixation task, even with orientation differences as large as 80°. When their participants attended to the stimuli, they showed that the sensitivity of channels processing the orientation of attended stimuli was at least twice as good as that of the mismatch channels.

The absence of a vMMN to contrast deviants corroborates the findings of Nyman et al. (1990), who also searched fruitlessly for one. Wei, Chan, and Luo (2002), however, concluded that there is a vMMN to contrast changes. But they did not control for the physical differences between lower and higher contrast stimuli as we and Nyman et al. did.

As far as we can tell, we are the first to test phase as a deviant feature for the vMMN. Phase information is essential in human vision. For example, Piotrowski and Campbell (1982) showed that one image's spatial frequency spectrum combined with the phase spectrum of a different image yields an image that looks like the latter and not at all like the former. But Piotrowski and Campbell also showed that this phenomenon survives with coarse encoding of phase, for example into only two levels. Consistent with this, psychophysical studies of phase discrimination show that highly trained observers can have thresholds ranging from about one-third of (Burr, 1980), to half of (Caelli & Bevan, 1982), to about equal to (Troscianko & Harris, 1988), the difference we used. In any case, our posttest results suggest our participants could see the phase changes.

We also failed to find a genuine vMMN to spatial frequency deviants. File et al. (2017) also failed to find such a vMMN to decreases in spatial frequency, admittedly of complex windmill patterns that also vary in orientation content. They did find a genuine vMMN when they increased spatial frequency in the same patterns, suggesting that it arises only if there is a combination of features that increase, in this case of orientation and spatial frequency. Others reporting spatial frequency vMMNs omitted any control for adaptation, hence reporting classic vMMNs (e.g., Kenemans, Jong, & Verbaten, 2003; Maekawa et al., 2005; Maekawa, Tobimatsu, Ogata, Onitsuka, & Kanba, 2009; Stagg et al., 2004).

One could argue that we did not find a genuine vMMN to any deviant feature because the multi-feature paradigm is not ideal for showing the vMMN. Although the multi-feature paradigm is well established in the auditory literature, the paradigm has been adopted in only a handful of vMMN experiments (e.g., Grimm, Bendixen, Deouell, & Schröger, 2009; He, Hu, Pakarinen, Li, & Zhou, 2014; Kreegipuu et al., 2013; Qian et al., 2014; Shi, Wu, Sun, Dang, & Zhao, 2013). It would be useful to compare when deviants appear in both a traditional oddball paradigm and a multi-feature paradigm with suitable controls. Given that Grimm et al. (2009) used the multi-feature paradigm to show a genuine vMMN to color, alignment, and shape, we suspect that we did not find a genuine vMMN because we manipulated single, low-level properties of visual input, whereas Grimm et al. manipulated properties that combine features (e.g., luminance with color).[3]

Although we did not find evidence for a vMMN, in further exploration of the data, we did find an early deviance-related positivity. According to our PCA, the components contributing to this early deviant-related positivity are the P1, anterior N1, and posterior N1. These differences are significant for the P1 and anterior N1 in all feature deviants, except for phase deviants. This could reflect phase invariance in complex cells in V1 (De Valois, Albrecht, & Thorell, 1982). Given these components are sensitive to stimulus type; we propose these deviant-related positivities may reflect the first instance of prediction error in vision. We discuss this further below but make clear that we did not predict such findings; therefore, they are exploratory.

4 | GENERAL DISCUSSION

We conducted two experiments to test whether low-level feature deviants yield the genuine vMMN. This is becoming increasingly important considering some inconsistent findings

[3]For example, to unconfound color from luminance, one would have had to measure each participant's isoluminance point prior to EEG testing (see Cavanagh, & Favreau, 1985 for a method) and then used each participant's value during his or her EEG testing.

in research into low-level deviance. In both experiments, we isolated and manipulated features of visual input based on our understanding of the visual system's physiology, we separated adaptation effects from genuine deviance detection, and we controlled for attention.

In Experiment 1, we replicated Kimura et al.'s (2009) method and incorporated three additional conditions to examine the effect of using Gabor patches, which match the spatial properties of V1 simple cells' receptive fields, versus bars, which do not so-well match those receptive fields, and the effects of attending to versus away from the stimulus of interest. No condition produced a genuine vMMN. We could not replicate the results of Kimura et al. (2009) and it is not likely we would be able to do so given their effect size and the statistical power of our experiment (= 0.99). Our Bayesian statistics show that it is reasonable to conclude that there is no genuine orientation vMMN.

We searched again for a genuine vMMN to changes in orientation, along with changes to other basic properties of visual stimuli, in Experiment 2. This time, we employed the multi-feature paradigm and cascadic control. We did not find a genuine vMMN for contrast, phase, and spatial frequency deviants. We replicated strong evidence for the null hypothesis for orientation deviants.

Although our findings are different from some existing research, we suspect that our rigorous design and controls have allowed us to isolate and determine the true effect of low-level deviance on the visual system. We propose that some experiments do not enact suitable controls for attention and adaptation (also determined by the stimulus used), whereas others do, which is why some experiments of low-level deviants show a vMMN, whereas others do not. Nevertheless, existing feature-deviance research has been vital to appreciate how the brain encodes and detects regularity and irregularity, respectively, even when attention is elsewhere. Our findings add to the appreciation of which types of visual deviants yield the genuine vMMN and why.

The eye-tracking data in Experiment 1 were essential in understanding why previous studies reported vMMNs. Our data are consistent with the notion that a genuine vMMN is more likely for deviants in which multiple dimensions of visual input change, suggesting that perhaps the vMMN is concerned with detecting deviants involving higher order features or feature-combinations encoded to perceptual objects.

If so, our findings point to a difference between the vMMN and the MMN: one of the principal features of the MMN is that it occurs in response to regularity violations in well-isolated, low-level, physiologically plausible, sensory features. It is possible that existing vMMN paradigms are not suited to test low-level deviants because the visual system is equally (if not more) concerned with spatial order than temporal order.

Another possibility is that the visual system detects low-level deviance in a process that is not revealed by the vMMN. We observed what might be an index for detecting low-level visual irregularities in both experiments: amplitudes were more positive for deviants compared to identical equiprobable controls at occipito-parieto-lateral electrodes between 80 and 200 ms. We found strong and converging evidence for deviance-related effects for the anterior N1 PCA component at occipital locations (i.e., with a positive deviant minus control difference potential) in both experiments and in all conditions with the only exception of phase in Experiment 2 (in which the evidence was inconclusive). We also found substantial evidence for deviance-related effects for the P1 and posterior N1 PCA components in some conditions. These were, however, not consistent across experiments and conditions and further research is needed to establish if these P1 and posterior N1 differences can be replicated.

If we accept that these early deviant-related positivities are meaningful, we could then consider these early positivities as the first instance of prediction error in vision perhaps comparable to the pre-MMN signals reported for the auditory middle-latency response. These early auditory responses are genuine (controlled for adaptation), positive (i.e., Pa at 30 ms, Slabu, Escera, Grimm, & Costa-Faidella, 2010), and negative (Nb at 40 ms) components that are sensitive to simple acoustic-feature irregularities (Alho, Grimm, Mateo-León, Costa-Faidella, & Escera, 2012; Althen, Grimm, & Escera, 2013; Grimm, Escera, Slabu, & Costa-Faidella, 2011; Leung, Cornella, Grimm, & Escera, 2012; Recasens, Grimm, Capilla, Nowak, & Escera, 2014). These components differ from the MMN in origin (Recasens et al., 2014) and in what evokes them. The latter is because simple auditory changes produce the response; whereas, complex irregularities, such as feature conjunctions, do not (Cornella, Leung, Grimm, & Escera, 2012).

Although there are reports of increased early positivity to deviants in visual input (e.g., Berti & Schröger, 2004; Chen, Huang, Luo, Peng, & Liu, 2010; Fu, Fan, & Chen, 2003; Kimura, Katayama, & Murohashi, 2006b; Müller et al., 2012; Sulykos, Kecskés-Kovács, & Czigler, 2013; Sysoeva, Lange, Sorokin, & Campbell, 2015), we believe we are the first to propose this early positivity as a marker for prediction error. Some have described this early positivity as a change-related positivity (Kimura, Katayama, & Murohashi, 2005, 2006a, 2006b, 2006c; Wang et al., 2003). However, this component is thought to reflect a mismatch between two stimuli rather than deviance or predictability—much like adaptation. To distinguish deviant-related positivity from change-related positivity one would need to isolate adaptation-related and deviant-related differences. That is what we have done. Ours is the first study to suggest that a deviant-related positivity is

a genuine deviance response free from adaptation, reflecting prediction error.

Pre-vMMN prediction error may have broader implications for how we conceptualize visual processing of unpredicted changes. It could be promising to investigate this pre-vMMN positivity further.

5 | CONCLUSIONS

Our results indicate that low-level feature deviants do not yield the vMMN if properly controlled for effects of adaptation, allocation of overt and covert attention, physiological plausibility, and isolation of manipulated feature. We surprisingly failed to replicate findings by Kimura et al. (2009) and discovered what appears to be a pre-vMMN positive index of deviance detection reserved for low-level changes in visual input. This may reflect differential processing for different visual changes and we encourage others to search for genuine pre-vMMN predictive processing.

ACKNOWLEDGMENTS

We are grateful to Melina Posch and Taavi Wenk who helped us to collect the data and Motohiro Kimura for giving us bitmaps of his stimuli from Kimura et al. (2009). Deutscher Akademischer Austausch Dienst (DAAD) Short-Term Grant number 91651341 supported AGM's visit to University of Leipzig. The project was funded by the German Research Foundation (DFG) with project number SCHR 375/25-1.

CONFLICT OF INTEREST

There are no conflicts of interest.

AUTHOR CONTRIBUTIONS

All authors contributed to the experiment's conception and design. AGM and AW contributed to programing, data acquisition, and data analysis. All authors contributed to the interpretation of the results. AGM wrote the first draft of the manuscript. All authors contributed to revisions.

OPEN ACCESS

Data from the two experiments are available on request to AW.

ORCID

Alie G. Male https://orcid.org/0000-0003-1247-2577
Robert P. O'Shea https://orcid.org/0000-0003-3132-7199
Erich Schröger https://orcid.org/0000-0002-8321-6629
Dagmar Müller https://orcid.org/0000-0001-9289-1215
Urte Roeber https://orcid.org/0000-0002-6631-5828
Andreas Widmann https://orcid.org/0000-0003-3664-8581

REFERENCES

Alho, K., Grimm, S., Mateo-León, S., Costa-Faidella, J., & Escera, C. (2012). Early processing of pitch in the human auditory system. *European Journal of Neuroscience*, *36*, 2972–2978. https://doi.org/10.1111/j.1460-9568.2012.08219.x

Althen, H., Grimm, S., & Escera, C. (2013). Simple and complex acoustic regularities are encoded at different levels of the auditory hierarchy. *European Journal of Neuroscience*, *38*, 3448–3455. https://doi.org/10.1111/ejn.12346

Astikainen, P., Lillstrang, E., & Ruusuvirta, T. (2008). Visual mismatch negativity for changes in orientation: A sensory memory-dependent response. *European Journal of Neuroscience*, *28*, 2319–2324. https://doi.org/10.1111/j.1460-9568.2008.06510.x

Astikainen, P., Ruusuvirta, T., Wikgren, J., & Korhonen, T. (2004). The human brain processes visual changes that are not cued by attended auditory stimulation. *Neuroscience Letters*, *368*, 231–234. https://doi.org/10.1016/j.neulet.2004.07.025

Auksztulewicz, R., & Friston, K. (2015). Attentional enhancement of auditory mismatch responses: A DCM/MEG study. *Cerebral Cortex*, *25*, 4273–4283. https://doi.org/10.1093/cercor/bhu323

Berti, S., & Schröger, E. (2004). Distraction effects in vision: Behavioral and event-related potential indices. *NeuroReport*, *15*, 665–669. https://doi.org/10.1097/01.wnr.0000116969.73984.bc

Bigdely-Shamlo, N., Mullen, T., Kothe, C., Su, K., & Robbins, K. A. (2015). The PREP pipeline: Standardized preprocessing for large-scale EEG analysis. *Frontiers in Neuroinformatics*, *9*(16), 1–20. https://doi.org/10.3389/fninf.2015.00016

Bodnár, F., File, D., Sulykos, I., Kecskés-Kovács, K., & Czigler, I. (2017). Automatic change detection in vision: Adaptation, memory mismatch, or both? II: Oddball and adaptation effects on event-related potentials. *Attention, Perception, & Psychophysics*, *79*, 2396–2411. https://doi.org/10.3758/s13414-017-1402-x

Brainard, D. H. (1997). The psychophysics toolbox. *Spatial Vision*, *10*, 433–436. Retrieved from http://bbs.bioguider.com/images/upfile/2006-4/200641014348.pdf

Burr, D. C. (1980). Sensitivity to spatial phase. *Vision Research*, *20*, 391–396. https://doi.org/10.1016/0042-6989(80)90029-2

Caelli, T., & Bevan, P. (1982). Visual sensitivity to two-dimensional spatial phase. *Journal of the Optical Society of America*, *72*, 1375–1381. https://doi.org/10.1364/JOSA.72.001375

Cammann, R. (1990). Is there a mismatch negativity (MMN) in visual modality? *Behavioral and Brain Sciences*, *13*, 234–235. https://doi.org/10.1017/S0140525X00078420

Cavanagh, P., & Favreau, O. E. (1985). Color and luminance share a common motion pathway. *Vision Research*, *25*, 1595–1601. https://doi.org/10.1016/0042-6989(85)90129-4

Chang, Y., Xu, J., Shi, N., Pang, X., Zhang, B., & Cai, Z. (2011). Dysfunction of preattentive visual information processing among patients with major depressive disorder. *Biological Psychiatry*, *69*, 742–747. https://doi.org/10.1016/j.biopsych.2010.12.024

Chaumon, M., Bishop, D. V. M., & Busch, N. A. (2015). A practical guide to the selection of independent components of the electroencephalogram for artifact correction. *Journal of Neuroscience Methods*, *250*, 47–63. https://doi.org/10.1016/j.jneumeth.2015.02.025

Chen, Y., Huang, X., Luo, Y., Peng, C., & Liu, C. (2010). Differences in the neural basis of automatic auditory and visual time perception:

ERP evidence from an across-modal delayed response oddball task. *Brain Research*, *1325*, 100–111. https://doi.org/10.1016/j.brainres.2010.02.040

Cleary, K. M., Donkers, F. C. L., Evans, A. M., & Belger, A. (2013). Investigating developmental changes in sensory processing: visual mismatch response in healthy children. *Frontiers in Human Neuroscience.*, *7*.

Cohen, J. (1977). *Statistical power analysis for the behavioral sciences* (Rev ed.). New York, NY: Academic Press.

Cornella, M., Leung, S., Grimm, S., & Escera, C. (2012). Detection of simple and pattern regularity violations occurs at different levels of the auditory hierarchy. *PLoS ONE*, *7*(8), 1–8. https://doi.org/10.1371/journal.pone.0043604

Czigler, I., Balázs, L., & Winkler, I. (2002). Memory-based detection of task-irrelevant visual changes. *Psychophysiology*, *39*, 869–873. https://doi.org/10.1017/S0048577202020218

Czigler, I., & Csibra, G. (1990). Event-related potentials in a visual discrimination task: Negative waves related to detection and attention. *Psychophysiology*, *27*, 669–676. https://doi.org/10.1111/j.1469-8986.1990.tb03191.x

Czigler, I., & Pató, L. (2009). Unnoticed regularity violation elicits change-related brain activity. *Biological Psychology.*, *80*(3), 339–347.

Czigler, I., & Sulykos, I. (2010). Visual mismatch negativity to irrelevant changes is sensitive to task-relevant changes. *Neuropsychologia*, *48*, 1277–1282. https://doi.org/10.1016/j.neuropsychologia.2009.12.029

Daugman, J. G. (1985). Uncertainty relation for resolution in space, spatial frequency, and orientation optimized by two-dimensional visual cortical filters. *Journal of the Optical Society of America A*, *2*, 1160–1169. https://doi.org/10.1364/JOSAA.2.001160

De Valois, R. L., Albrecht, D. G., & Thorell, L. G. (1982). Spatial frequency selectivity of cells in macaque visual cortex. *Vision Research*, *22*, 545–559. https://doi.org/10.1016/0042-6989(82)90113-4

Delorme, A., & Makeig, S. (2004). EEGLAB: An open source toolbox for analysis of single-trial EEG dynamics including independent component analysis. *Journal of Neuroscience Methods*, *134*, 9–21. https://doi.org/10.1016/j.jneumeth.2003.10.009

Delorme, A., Palmer, J., Onton, J., Oostenveld, R., & Makeig, S. (2012). Independent EEG sources are dipolar. *PLoS ONE*, *7*(2), e30135. https://doi.org/10.1371/journal.pone.0030135

Dien, J., Khoe, W., & Mangun, G. R. (2007). Evaluation of PCA and ICA of simulated ERPs: Promax versus Infomax rotations. *Human Brain Mapping*, *28*, 742–763. https://doi.org/10.1002/hbm.20304

Farkas, K., Stefanics, G., Marosi, C., & Csukly, G. (2015). Elementary sensory deficits in schizophrenia indexed by impaired visual mismatch negativity. *Schizophrenia Research*, *166*, 164–170. https://doi.org/10.1016/j.schres.2015.05.011

Faul, F., Erdfelder, E., Buchner, A., & Lang, A.-G. (2009). Statistical power analyses using G*Power 3.1: Tests for correlation and regression analyses. *Behavior Research Methods*, *41*, 1149–1160. https://doi.org/10.3758/BRM.41.4.1149

Faul, F., Erdfelder, E., Lang, A., & Buchner, A. (2007). G*Power 3: A flexible statistical power analysis program for the social, behavioral, and biomedical sciences. *Behavior Research Methods*, *39*, 175–191. https://doi.org/10.3758/bf03193146

Field, D. J., & Tolhurst, D. J. (1986). The structure and symmetry of simple-cell receptive-field profiles in the cat's visual cortex. *Proceedings of the Royal Society of London. Series B, Biological Sciences*, *228*, 379–400. Retrieved from https://www.jstor.org/stable/36176

File, D., File, B., Bodnár, F., Sulykos, I., Kecskés-Kovács, K., & Czigler, I. (2017). Visual mismatch negativity (vMMN) for low- and high-level deviances: A control study. *Attention, Perception, & Psychophysics*, *79*, 2153–2170. https://doi.org/10.3758/s13414-017-1373-y

Fredericksen, R. E., Bex, P. J., & Verstraten, F. A. J. (1998). How big is a Gabor patch, and why should we care? *Journal of the Optical Society of America A*, *15*(1), 1–12. https://doi.org/10.1364/JOSAA.15.001959

Fu, S., Fan, S., & Chen, L. (2003). Event-related potentials reveal involuntary processing of orientation changes in the visual modality. *Psychophysiology*, *40*, 770–775. https://doi.org/10.1111/1469-8986.00077

Garrido, M. I., Kilner, J. M., Stephan, K. E., & Friston, K. J. (2009). The mismatch negativity: A review of underlying mechanisms. *Clinical Neurophysiology*, *120*, 453–463. https://doi.org/10.1016/j.clinph.2008.11.029

Graham, N. V. S. (1989). *Visual pattern analyzers*. New York, NY: Oxford University Press.

Grimm, S., Bendixen, A., Deouell, L. Y., & Schröger, E. (2009). Distraction in a visual multi-deviant paradigm: Behavioral and event-related potential effects. *International Journal of Psychophysiology*, *72*, 260–266. https://doi.org/10.1016/j.ijpsycho.2009.01.005

Grimm, S., Escera, C., Slabu, L. M., & Costa-Faidella, J. (2011). Electrophysiological evidence for the hierarchical organization of auditory change detection in the human brain. *Psychophysiology*, *48*, 377–384. https://doi.org/10.1111/j.1469-8986.2010.01073.x

Groppe, D. M., Makeig, S., & Kutas, M. (2009). Identifying reliable independent components via split-half comparisons. *NeuroImage*, *45*, 1199–1211. https://doi.org/10.1016/j.neuroimage.2008.12.038

He, J., Hu, Y., Pakarinen, S., Li, B., & Zhou, Z. (2014). Different effects of alcohol on automatic detection of color, location and time change: A mismatch negativity study. *Journal of Psychopharmacology*, *28*, 1109–1114. https://doi.org/10.1177/0269881114548294

Hedge, C., Stothart, G., Jones, J. T., Frías, P. R., Magee, K. L., & Brooks, J. C. W. (2015). A frontal attention mechanism in the visual mismatch negativity. *Behavioral Brain Research*, *293*, 173–181. https://doi.org/10.1016/j.bbr.2015.07.022

Horn, J. L. (1965). A rationale and test for the number of factors in factor analysis. *Psychometrika*, *30*, 179–185. https://doi.org/10.1007/BF02289447

Horváth, J., Czigler, I., Jacobsen, T., Maess, B., Schröger, E., & Winkler, I. (2008). MMN or no MMN: No magnitude of deviance effect on the MMN amplitude. *Psychophysiology*, *45*, 60–69. https://doi.org/10.1111/j.1469-8986.2007.00599.x

Kekoni, J., Hämäläinen, H., Saarinen, M., Gröhn, J., Reinikainen, K., Lehtokoski, A., & Näätänen, R. (1997). Rate effect and mismatch responses in the somatosensory system: ERP-recordings in humans. *Biological Psychology*, *46*, 125–142. https://doi.org/10.1016/S0301-0511(97)05249-6

Kenemans, J. L., Hebly, W., van den Heuvel, E., & Grent-'T-Jong, T. (2010). Moderate alcohol disrupts a mechanism for detection of rare events in human visual cortex. *Journal of Psychopharmacology*, *24*, 839–845. https://doi.org/10.1177/0269881108098868

Kenemans, J. L., Jong, T. G., & Verbaten, M. N. (2003). Detection of visual change: Mismatch or rareness? *NeuroReport*, *14*, 1239–1242. https://doi.org/10.1097/01.wnr.0000081871.45938.c4

Kimura, M., Katayama, J., & Murohashi, H. (2005). Positive difference in ERPs reflects independent processing of visual changes. *Psychophysiology*, *42*, 369–379. https://doi.org/10.1111/j.1469-8986.2005.00297.x

Kimura, M., Katayama, J., & Murohashi, H. (2006a). An ERP study of visual change detection: Effects of magnitude of spatial frequency changes on the change-related posterior positivity. *International Journal of Psychophysiology*, *62*, 14–23. https://doi.org/10.1016/j.ijpsycho.2005.11.005

Kimura, M., Katayama, J., & Murohashi, H. (2006b). Independent processing of visual stimulus changes in ventral and dorsal stream features indexed by an early positive difference in event-related brain potentials. *International Journal of Psychophysiology*, *59*, 141–150. https://doi.org/10.1016/j.ijpsycho.2005.03.023

Kimura, M., Katayama, J., & Murohashi, H. (2006c). Probability-independent and -dependent ERPs reflecting visual change detection. *Psychophysiology*, *43*, 180–189. https://doi.org/10.1111/j.1469-8986.2006.00388.x

Kimura, M., Katayama, J., Ohira, H., & Schröger, E. (2009). Visual mismatch negativity: New evidence from the equiprobable paradigm. *Psychophysiology*, *46*, 402–409. https://doi.org/10.1111/j.1469-8986.2008.00767.x

Kimura, M., & Takeda, Y. (2015). Automatic prediction regarding the next state of a visual object: Electrophysiological indicators of prediction match and mismatch. *Brain Research*, *1626*, 31–44. https://doi.org/10.1016/j.brainres.2015.01.013

Kleiner, M. (2013). *Introduction to Psychtoolbox-3*. Retrieved from https://github.com/Psychtoolbox-3/Psychtoolbox-3/blob/master/Psychtoolbox/PsychDocumentation/PTBTutorial-ECVP2013.pdf

Kolb, H., Fernandez, E., & Nelson, R. (2018, December 4). *WEBVISION: The organization of the retina and visual system*. Retrieved from http://www.webvision.med.utah.edu

Krauel, K., Schott, P., Sojka, B., Pause, B. M., & Ferstl, R. (1999). Is there a mismatch negativity analogue in the olfactory event-related potential? *Journal of Psychophysiology*, *13*, 49–55. https://doi.org/10.1027//0269-8803.13.1.49

Kreegipuu, K., Kuldkepp, N., Sibolt, O., Toom, M., Allik, J., & Näätänen, R. (2013). vMMN for schematic faces: Automatic detection of change in emotional expression. *Frontiers in Human Neuroscience*, *7*(714), 1–11. https://doi.org/10.3389/fnhum.2013.00714

Kujala, T., Tervaniemi, M., & Schröger, E. (2007). The mismatch negativity in cognitive and clinical neuroscience: Theoretical and methodological considerations. *Biological Psychology*, *74*(1), 1–19. https://doi.org/10.1016/j.biopsycho.2006.06.001

Lee, M. D., & Wagenmakers, E.-J. (2013). *Bayesian cognitive modeling: A practical course*. Cambridge, UK: Cambridge University Press. https://doi.org/10.1017/CBO9781139087759

Leung, S., Cornella, M., Grimm, S., & Escera, C. (2012). Is fast auditory change detection feature-specific? An electrophysiological study in humans. *Psychophysiology*, *49*, 933–942. https://doi.org/10.1111/j.1469-8986.2012.01375.x

Li, X., Liang, Z., Kliener, M., & Lu, Z. (2010). RTbox: A device for highly accurate response time measurements. *Behavior Research Methods*, *2010*(42), 212–225. https://doi.org/10.3758/BRM.42.1.212

Lopez-Calderon, J., & Luck, S. J. (2014). ERPLAB: An open-source toolbox for the analysis of event-related potentials. *Frontiers in Human Neuroscience*, *8*(213), 1–14. https://doi.org/10.3389/fnhum.2014.00213

Maekawa, T., Goto, Y., Kinukawa, N., Taniwaki, T., Kanba, S., & Tobimatsu, S. (2005). Functional characterization of mismatch negativity to a visual stimulus. *Clinical Neurophysiology*, *116*, 2392–2402. https://doi.org/10.1016/j.clinph.2005.07.006

Maekawa, T., Katsuki, S., Kishimoto, J., Onitsuka, T., Ogata, K., Yamasaki, T., … Kanba, S. (2013). Altered visual information processing systems in bipolar disorder: Evidence from visual MMN and P3. *Frontiers in Human Neuroscience*, *7*(403), 1–11. https://doi.org/10.3389/fnhum.2013.00403

Maekawa, T., Tobimatsu, S., Ogata, K., Onitsuka, T., & Kanba, S. (2009). Preattentive visual change detection as reflected by the mismatch negativity (MMN): Evidence for a memory-based process. *Neuroscience Research*, *65*, 107–112. https://doi.org/10.1016/j.neures.2009.06.005

Makeig, S., Bell, A. J., Jung, T. P., & Sejnowski, T. J. (1996). Independent component analysis of electroencephalographic data. *Advances in Neural Information Processing Systems*, *8*, 145–151. Retrieved from https://papers.nips.cc/paper/1091-independent-component-analysis-of-electroencephalographic-data.pdf

Mathôt, S. (2017). *Bayes like a Baws: Interpreting Bayesian repeated measures in JASP*. Retrieved from https://www.cogsci.nl/blog/interpreting-bayesian-repeated-measures-in-jasp

May, P. J., & Tiitinen, H. (2010). Mismatch negativity (MMN), the deviance-elicited auditory deflection, explained. *Psychophysiology*, *46*, 1–57. https://doi.org/10.1111/j.1469-8986.2009.00856.x

Mognon, A., Jovicich, J., Bruzzone, L., & Buiatti, M. (2011). ADJUST: An automatic EEG artifact detector based on the joint use of spatial and temporal features. *Psychophysiology*, *48*, 229–240. https://doi.org/10.1111/j.1469-8986.2010.01061.x

Müller, D., Roeber, U., Winkler, I., Trujillo-Barreto, N., Czigler, I., & Schröger, E. (2012). Impact of lower- vs. upper-hemifield presentation on automatic color-deviance detection: A visual mismatch negativity study. *Brain Research*, *1472*, 89–98. https://doi.org/10.1016/j.brainres.2012.07.016

Näätänen, R. (1992). Event-related potentials and automatic information processing. In R. Näätänen (Ed.), *Attention and brain function* (pp. 102–296). Hillsdale, NJ: Lawrence Erlbaum Associates.

Näätänen, R., Gaillard, A. W. K., & Mäntysalo, S. (1978). Early selective-attention effect on evoked potential reinterpreted. *Acta Psychologica*, *42*, 313–329. https://doi.org/10.1016/0001-6918(78)90006-9

Näätänen, R., Jacobsen, T., & Winkler, I. (2005). Memory-based or afferent processes in mismatch negativity (MMN): A review of the evidence. *Psychophysiology*, *42*, 25–32. https://doi.org/10.1111/j.1469-8986.2005.00256.x

Näätänen, R., Paavilainen, P., Rinne, T., & Alho, K. (2007). The mismatch negativity (MMN) in basic research of central auditory processing: A review. *Clinical Neurophysiology*, *118*, 2544–2590. https://doi.org/10.1016/j.clinph.2007.04.026

Näätänen, R., Pakarinen, S., Rinne, T., & Takegata, R. (2004). The mismatch negativity (MMN): Towards the optimal paradigm. *Clinical Neurophysiology*, *115*, 140–144. https://doi.org/10.1016/j.clinph.2003.04.001

Nyman, G., Alho, K., Laurinen, P., Paavilainen, P., Radil, T., Reinikainen, K., … Näätänen, R. (1990). Mismatch negativity (MMN) for sequences of auditory and visual stimuli: Evidence for a mechanism specific to the auditory modality. *Electroencephalography and Clinical Neurophysiology*, *77*, 436–444. Retrieved from https://www.ncbi.nlm.nih.gov/pubmed/1701706

O'Shea, R. P. (2015). Refractoriness about adaptation. *Frontiers in Human Neuroscience*, *9*(38), 1–3. https://doi.org/10.3389/fnhum.2015.00038

Paavilainen, P., Alho, K., Reinikainen, K., Sams, M., & Näätänen, R. (1991). Right hemisphere dominance of different mismatch negativities. *Electroencephalography and Clinical Neurophysiology*, *78*, 466–479. https://doi.org/10.1016/0013-4694(91)90064-B

Pelli, D. G. (1997). The VideoToolbox software for visual psychophysics: Transforming numbers into movies. *Spatial Vision*, *10*, 437–442. https://doi.org/10.1163/156856897X00366

Perrin, F., Pernier, J., Bertnard, O., Giard, M. H., & Echallier, J. F. (1987). Mapping of scalp potentials by surface spline interpolation. *Electroencephalography and Clinical Neurophysiology*, *66*, 75–81. https://doi.org/10.1016/0013-4694(87)90141-6

Piotrowski, L. N., & Campbell, F. W. (1982). A demonstration of the visual importance and flexibility of spatial frequency amplitude and phase. *Perception*, *11*, 337–346. https://doi.org/10.1068/p110337

Qian, X., Liu, Y. I., Xiao, B., Gao, L. I., Li, S., Dang, L., … Zhao, L. (2014). The visual mismatch negativity (vMMN): Toward the optimal paradigm. *International Journal of Psychophysiology*, *93*, 311–315. https://doi.org/10.1016/j.ijpsycho.2014.06.004

Quiroga, R. Q., & Pedreira, C. (2011). How do we see art: An eye-tracker study. *Frontiers in Human Neuroscience*, *5*, 98–98. https://doi.org/10.3389/fnhum.2011.00098

Recasens, M., Grimm, S., Capilla, A., Nowak, R., & Escera, C. (2014). Two sequential processes of change detection in hierarchically ordered areas of the human auditory cortex. *Cerebral Cortex*, *24*, 1047–3211. https://doi.org/10.1093/cercor/bhs295

Regan, D., & Price, P. (1986). Periodicity in orientation discrimination and the unconfounding of visual information. *Vision Research*, *26*, 1299–1302. https://doi.org/10.1016/0042-6989(86)90111-2

Ruhnau, P., Herrmann, B., & Schröger, E. (2012). Finding the right control: The mismatch negativity under investigation. *Clinical Neurophysiology*, *123*, 507–512. https://doi.org/10.1016/j.clinph.2011.07.035

Schröger, E., & Wolff, C. (1996). Mismatch response of the human brain to changes in sound location. *NeuroReport*, *7*, 3005–3008. Retrieved from https://www.ncbi.nlm.nih.gov/pubmed/9116228

Shi, L. P., Wu, J., Sun, G., Dang, L. J., & Zhao, L. (2013). Visual mismatch negativity in the "optimal" multi-feature paradigm. *Journal of Integrative Neuroscience*, *12*, 247–258. https://doi.org/10.1142/S0219635213500179

Slabu, L. M., Escera, C., Grimm, S., & Costa-Faidella, J. (2010). Early change detection in humans as revealed by auditory brainstem and middle-latency evoked potentials. *European Journal of Neuroscience*, *32*, 859–865. https://doi.org/10.1111/j.1460-9568.2010.07324.x

Smout, C. A., Tang, M. F., Garrido, M. I., & Mattingley, J. B. (2019). Attention promotes the neural encoding of prediction errors. *PLOS Biology*, *17*(2), 1–22. https://doi.org/10.1371/journal.pbio.2006812

Snowden, R. J., & Hammett, S. T. (1998). The effects of surround contrast on contrast thresholds, perceived contrast and contrast discrimination. *Vision Research*, *38*, 1935–1945. https://doi.org/10.1016/S0042-6989(97)00379-9

Spence, C. (2019). Reading the plate. *International Journal of Gastronomy and Food Science*, *16*(100156), 1–7. https://doi.org/10.1016/j.ijgfs.2019.100156

Stagg, C., Hindley, P., Tales, A., & Butler, S. (2004). Visual mismatch negativity: The detection of stimulus change. *NeuroReport*, *15*, 659–663. https://doi.org/10.1097/01.wnr.0000116966.73984.58

Stanislaw, H., & Todorov, N. (1999). Calculation of signal detection theory measures. *Behavior Research Methods, Instruments, & Computers.*, *31*(1), 137–149.

Stothart, G., & Kazanina, N. (2013). Oscillatory characteristics of the visual mismatch negativity: what evoked potentials aren't telling us. *Frontiers in Human Neuroscience.*, *7*.

Sulykos, I., & Czigler, I. (2011). One plus one is less than two: Visual features elicit non-additive mismatch-related brain activity. *Brain Research.*, *1398*, 64–71.

Sulykos, I., Kecskés-Kovács, K., & Czigler, I. (2013). Mismatch negativity does not show evidence of memory reactivation in the visual modality. *Journal of Psychophysiology*, *27*(1), 1–6. https://doi.org/10.1027/0269-8803/a000085

Sussman, E. S., Chen, S., Sussman-Fort, J., & Dinces, E. (2014). The Five Myths of MMN: Redefining How to Use MMN in Basic and Clinical Research. *Brain Topography.*, *27*(4), 553–564.

Sysoeva, O. V., Lange, E. B., Sorokin, A. B., & Campbell, T. (2015). From pre-attentive processes to durable representation: An ERP index of visual distraction. *International Journal of Psychophysiology.*, *95*(3), 310–321.

Takács, E., Sulykos, I., Czigler, I., Barkaszi, I., & Balázs, L. (2013). Oblique effect in visual mismatch negativity. *Frontiers in Human Neuroscience*, *7*, 591–594. https://doi.org/10.3389/fnhum.2013.00591

Troscianko, T., & Harris, J. (1988). Phase discrimination in chromatic compound gratings. *Vision Research*, *28*, 1041–1049. https://doi.org/10.1016/0042-6989(88)90081-8

Verhagen, J., & Wagenmakers, E. J. (2014). Bayesian tests to quantify the result of a replication attempt. *Journal of Experimental Psychology. General*, *143*, 1457–1475. https://doi.org/10.1037/a0036731

Wang, Y., Tian, S., Wang, H., Cui, L., Zhang, Y., & Zhang, X. (2003). Event-related potentials evoked by multi-feature conflict under different attentive conditions. *Experimental Brain Research.*, *148*(4), 451–457.

Webster, M. A., De Valois, K. K., & Switkes, E. (1990). Orientation and spatial frequency discrimination for luminance and chromatic gratings. *Journal of the Optical Society of America A*, *7*, 1034–1049. https://doi.org/10.1364/JOSAA.7.001034

Wei, J., Chan, T., & Luo, Y. (2002). A modified oddball paradigm "cross-modal delayed response" and the research on mismatch negativity. *Brain Research Bulletin*, *57*, 221–230. https://doi.org/10.1016/S0361-9230(01)00742-0

Winkler, I., Debener, S., Muller, K., & Tangermann, M. (2015). On the influence of high-pass filtering on ICA-based artifact reduction in EEG-ERP. In *Proceedings of the Annual International Conference of the IEEE Engineering in Medicine and Biology Society* (pp. 4101−4105). https://doi.org/10.1109/EMBC.2015.7319296

Winkler, I., Karmos, G., & Näätänen, R. (1996). Adaptive modeling of the unattended acoustic environment reflected in the mismatch negativity event-related potential. *Brain Research*, *742*, 239–252. https://doi.org/10.1016/S0006-8993(96)01008-6

Woldorff, M. G., Hackley, S. A., & Hillyard, S. A. (1991). The effects of channel-selective attention on the mismatch negativity wave elicited by deviant tones. *Psychophysiology*, *28*, 30–42. https://doi.org/10.1111/j.1469-8986.1991.tb03384.x

Woldorff, M. G., & Hillyard, S. A. (1990). Attentional influence on the mismatch negativity. *Behavioral and Brain Sciences*, *13*, 258–260. https://doi.org/10.1017/s0140525x00078699

Yan, T., Feng, Y., Liu, T., Wang, L., Mu, N., Dong, X., … Zhao, L. (2017). Theta oscillations related to orientation recognition in unattended condition: A vMMN study. *Frontiers in Behavioral Neuroscience*, *11*(166), 1–8. https://doi.org/10.3389/fnbeh.2017.00166

SUPPORTING INFORMATION

Additional Supporting Information may be found online in the Supporting Information section.

Figure S1 ERPs and difference waves from Experiment 1 processed with Kimura et al.'s (2009) pipeline. A. ERPs from the electrodes either identical with or interpolated to those of Kimura et al. B. Difference waves for the same electrodes as in A.

Table S1 Statistical results in the 100- to 150-ms mean-amplitude time window from the bar-edge condition data reanalyzed using Kimura et al.'s (2009) pre-processing pipeline. Frequentist *t* test *t* and *p* values, and Bayesian replication (BF_{r0}) and directed (BF_{-0}) *t* tests of differences in mean amplitudes (μV) for the tests reported by Kimura et al. at the same or interpolated electrode locations.

Table S2 Statistical results in the 200- to 250-ms mean-amplitude time window from the bar-edge condition data reanalyzed using Kimura et al.'s (2009) pre-processing pipeline. Frequentist *t* test *t* and *p* values, and Bayesian replication (BF_{r0}) and directed (BF_{-0}) *t* tests of differences in mean amplitudes (μV) for the tests reported by Kimura et al. at the same electrode locations.

How to cite this article: Male AG, O'Shea RP, Schröger E, Müller D, Roeber U, Widmann A. The quest for the genuine visual mismatch negativity (vMMN): Event-related potential indications of deviance detection for low-level visual features. *Psychophysiology*. 2020;00:e13576. https://doi.org/10.1111/psyp.13576